Geochemistry Geophysics Geosystems G3
AN ELECTRONIC JOURNAL OF THE EARTH SCIENCES
Published by AGU and the Geochemical Society

Article
Volume 7, Number 4
27 April 2006
Q04016, doi:10.1029/2005GC001090
ISSN: 1525-2027

Controls on back-arc basin formation

Maria Sdrolias and R. Dietmar Müller

EarthByte Group and School of Geosciences, University of Sydney, Building H11, New South Wales 2006, Australia (marias@geosci.usyd.edu.au; dietmar@geosci.usyd.edu.au)

[1] The relationship between subduction and back-arc spreading has been well known since the early days of plate tectonics. However, the reasons why back-arc basins are associated with some subduction systems but not all has remained elusive. We examine the kinematic controls on subduction and back-arc basins for both the present-day and Cenozoic to differentiate between the major competing hypotheses for back-arc basin formation and to explain their temporal and spatial distribution. Our new data set of subduction and back-arc basin parameters uses a new set of paleo-oceanic age grids (Müller et al., 2005) associated with a moving Atlantic-Indian Ocean hot spot reference frame (O'Neill et al., 2005). The plate model includes detailed reconstructed spreading histories of back-arc basins based on marine geophysical and satellite gravity data. Our combined rotation and oceanic paleo-age model provides the age distribution of subducting lithosphere through space and time, convergence rates, and the absolute motion of the downgoing and overriding plates. We find that back-arc basins develop when the age of subducting normal oceanic lithosphere is greater than 55 million years. Additionally, we establish an age-dip relationship showing that the intermediate dip angle of the subducting slab is always greater than 30° with back-arc spreading. Our results suggest that back-arc basin formation is always preceded by an absolute motion of the overriding plate away from the subduction hinge, thereby creating accommodation space between the overriding and subducting plates. Once back-arc extension is established, it continues regardless of overriding plate motion, indicating back-arc spreading is not a simple consequence of overriding plate behaviour. The landward migration of the overriding plate as a precursor to back-arc extension may indicate that extension on the overriding plate is influenced by the oceanward lateral flow of the mantle. However, once back-arc extension is established, rollback of the subduction hinge appears to be the primary force responsible for the continued creation of accommodation space. Our analysis indicates the driving mechanism for back-arc extension is a combination of surface kinematics, properties of the downgoing slab, the effect of lateral mantle flow on the slab, and mantle wedge dynamics.

Components: 17,713 words, 30 figures.

Keywords: back-arc basin; convergence; rollback; subduction.

Index Terms: 3001 Marine Geology and Geophysics: Back-arc basin processes; 3040 Marine Geology and Geophysics: Plate tectonics (8150, 8155, 8157, 8158); 3060 Marine Geology and Geophysics: Subduction zone processes (1031, 3613, 8170, 8413).

Received 28 July 2005; **Revised** 17 November 2005; **Accepted** 16 February 2006; **Published** 27 April 2006.

Sdrolias, M., and R. D. Müller (2006), Controls on back-arc basin formation, *Geochem. Geophys. Geosyst.*, *7*, Q04016, doi:10.1029/2005GC001090.

1. Introduction

[2] Back-arc basins form an integral but often neglected part of the subduction factory and are crucial to understanding the development and behaviour of subduction zones and associated mantle dynamics. Back-arc basins are defined as regions of extension at convergent plate margins where rifting and in some cases, seafloor spreading develops on the overriding plate. The occurrence of an

extensional stress regime adjacent to an area of major convergence, accretion and thrusting has often been considered counterintuitive and not easily explained by plate tectonic theory. Moreover, the reasons why not all subduction systems develop back-arc extension even though back-arc extension only occurs associated with subduction have never been adequately addressed. Several studies have attempted to address these fundamental issues by evoking either a thermal, mechanical and/or kinematic processes for the formation of back-arc basins [see *Stern*, 2002]. Is back-arc extension driven by the rollback of the subduction hinge caused by the negative buoyancy of the subducting slab which is a function of the age of the subducting lithosphere [*Elsasser*, 1971; *Molnar and Atwater*, 1978; *Dewey*, 1980; *Faccenna et al.*, 2001; *Hall et al.*, 2003; *Schellart et al.*, 2003]? Is the development of back-arc extension purely driven by the absolute motion of the overriding plate [*Chase*, 1978; *Scholz and Campos*, 1995]? Is the sea anchor force (a force exerted on the slab which resists its lateral motion) the only force responsible for back-arc spreading [*Scholz and Campos*, 1995]? Or is the development of back-arc extension independent of the surface kinematics and instead dominated by magmatism in the mantle wedge by rising diapirs [*Karig*, 1971] or secondary convection cells [*Sleep and Toksoz*, 1971]?

[3] More recently, analogue and numerical experiments to model subduction and the dynamic effect of back-arc spreading have shown the importance of hinge rollback in the development of subduction and back-arc spreading [*Faccenna et al.*, 2001; *Schellart et al.*, 2002; *Hall et al.*, 2003; *Schellart et al.*, 2003]. Analogue experiments of the Mediterranean region [*Faccenna et al.*, 2001] where several episodes of back-arc extension have developed found that back-arc spreading is accompanied by rapid rollback of the subduction hinge and steepening of the subducting slab. Similarly, the analogue models of *Schellart et al.* [2002, 2003] for the North Fiji Basin and Kuril Basin, respectively, require rapid rollback of the subduction hinge to open the back-arc plate and explain the observed deformation structures.

[4] The first numerical model to dynamically predict the onset of back-arc extension in an area dominated by regional compression [*Hall et al.*, 2003] determined that rapid extension on the overriding plate was driven by the rollback of the subduction hinge which arises when the vertical velocity of the downgoing slab exceeds the convergence rate. This is accompanied by a steepening of the subducting slab, thinning of the overriding plate and the establishment of a back-arc spreading system. The process of back-arc extension continues as a result of trench rollback.

[5] Studies relating upper plate stress with various present-day subduction zone parameters [*Jarrard*, 1986; *Heuret and Lallemand*, 2005; *Lallemand et al.*, 2005] have found that a relationship exists between the dip of the subducting slab and the presence/absence of back-arc extension or compression.

[6] In this study, we aim to differentiate between the major competing hypotheses by examining, for the first time, both present-day and paleo subduction and back-arc basin parameters in concert. Previous analysis of subduction and back-arc basin parameters have been confined to observational data from the present-day, many of which are currently outdated and known to be inaccurate. We derive a novel set of model predictions from our paleo-oceanic age and absolute plate motion model. Our plate model uses the new absolute reference frame of *O'Neill et al.* [2005] which is based on moving Atlantic-Indian ocean hot spots. The plate model also includes tighter constraints on the spreading histories between the major plates, including the motion between East and West Antarctica [*Cande et al.*, 2000] and the incorporation of back-arc basin plates [*Sdrolias et al.*, 2003; *Gaina and Müller*, 2004; *Sdrolias et al.*, 2004b], which were not utilized in previous global plate motion models. We have created a set of paleo-oceanic age grids based on the work by *Gaina and Müller* [2004] and *Müller et al.* [2005], which shows the age distribution of the seafloor through time and hence the age of the subducting lithosphere at each subduction zone. The convergence rate and direction along all subduction boundaries were created as well as the absolute motion of the overriding plate, including the back-arc basin plate. These parameters can be related to the presence/absence of back-arc extension and the behavior of the subducting slab. Using these back-arc and subduction zone parameters, we calculate the rollback speed of the subduction hinge at each subduction zone to assess its role in back-arc basin formation.

[7] We confined our study to eight selected subduction systems: the Tonga-Kermadec, Java-Sunda, Izu-Bonin-Mariana, Japan-Kuril, Aleutian, Cascadia, Middle America and Andes trenches

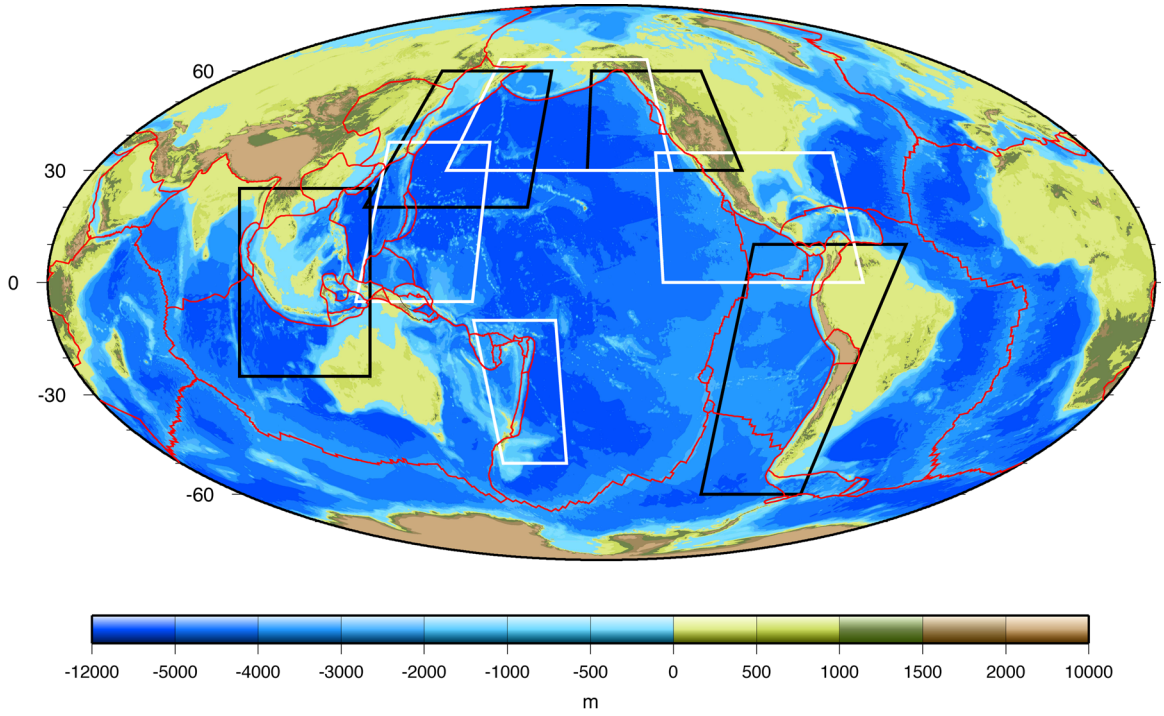

Figure 1. Mollweide projection of global bathymetry (ETOPO5) and topography (GTOPO). Present-day plate boundaries are marked in red and taken from the *Bird* [2003] data set. Alternating black and white boxes correspond to the selected regions of study and define the bounding boxes in Figures 2–9.

(Figure 1). These subduction systems were chosen as they satisfied several criteria: (1) They border the major oceanic basins where tight constraints on the motion history of the downgoing plate are available. (2) They are not associated with the subduction of anomalous materials such as very young oceanic crust, large volumes of continental, hybrid or volcanic arc crust; normal oceanic crust is almost exclusively subducted in our selected subduction zones. (3) They do not subduct anomalous back-arc basin crust which possess different physical, thermal and mechanical properties to normal oceanic crust. (4) The motion history of the overriding plate is well constrained, including the back-arc basin plates. (5) They are long-lived subduction systems [see *Gurnis et al.*, 2004] permitting a detailed analysis of past subduction activity over a period of time.

[8] The subduction systems within SE Asia and northeast of Australia (e.g., Philippine, Nankai, Ryukyu, Luzon, North Solomons, New Hebrides), the Sandwich and Caribbean trenches in the Atlantic as well as the Mediterranean were excluded from our study. In SE Asia, the subduction systems are young, short-lived and often subduct back-arc basin crust. The region is also riddled with continental and volcanic arc fragments. The Sandwich and Caribbean subduction systems do not have well constrained motion histories for the overriding plate. The Mediterranean subduction system is complicated by the present-day subduction of continental crust from the African plate.

[9] Although previous studies have included subduction zones that subduct back-arc basin crust in their analysis of subduction zone parameters [e.g., *Jarrard*, 1986; *Scholz and Campos*, 1995; *Lallemand et al.*, 2005], we do not believe that these systems which subduct lithosphere of different physical, thermal and mechanical properties to normal oceanic lithosphere are beneficial for investigating the relationship of back-arc basins with subduction of normal ocean crust.

2. Age of the Subducting Lithosphere

[10] The age of oceanic lithosphere subducting at the active trench is assumed to have a major influence over the style of subduction, the behavior of the subducted slab and the surface expression of this subduction on the overriding plate. Newly created oceanic lithosphere cools, subsides and thickens with increasing distance from the spreading axis due to thermal contraction. The density of the lithosphere increases as a function of its age

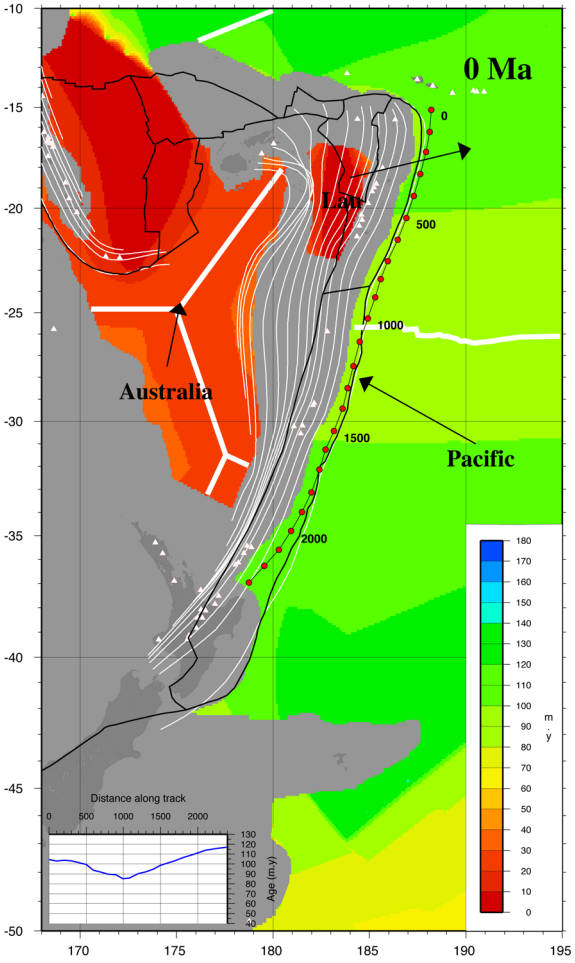

Figure 2a. Present-day age grid of the Tonga-Kermadec subduction system. Red and white triangles are present-day volcanoes and mark the active volcanic front. White lines mark the slab depth contours (in 100 km intervals) of *Gudmundsson and Sambridge* [1998] used in dip of slab calculations. Black arrows indicate the absolute plate velocity (rate and direction). Grey regions correspond to all nonoceanic crust, including continental crust, volcanic arcs, and oceanic plateaus. Thin black lines mark the present-day plate boundaries of *Bird* [2003]. Thick white line denotes the extinct plate boundary of the Osbourn Trough and South Fiji Basin spreading ridge. Thin black line with red circles denotes the strike of the trench with each red circle marking the distance along track. Each 500 km point is annotated. The small graph is a profile of the age of the subducting lithosphere along the strike of the trench.

while it cools and contracts and becomes less buoyant. Relationships between age and thickness [*Heestand and Crough*, 1981; *Stein and Stein*, 1996], age and trench depth [*Grellet and Dubois*, 1982], age and heat flow [*Sclater*, 1972; *Stein and Stein*, 1992] and age and depth of oceanic lithosphere [*Parsons and Sclater*, 1977; *Stein and Stein*, 1992] demonstrate the variations in character of the oceanic lithosphere depending upon its age. As a result, the way in which oceanic crust of different ages is subducted at oceanic trenches and the processes that occur on the overriding plate will differ. For example, an important distinction between the subduction of old and young oceanic lithosphere is the presence/absence of back-arc spreading on the overriding plate [*Uyeda*, 1977; *Uyeda and Kanamori*, 1979]. *Uyeda* [1977] and *Uyeda and Kanamori* [1979] noted that the eastern Pacific margin is presently subducting young oceanic lithosphere and back-arc basins have not formed on the overriding plate whereas the western Pacific margin is presently subducting old oceanic lithosphere and back-arc spreading is actively occurring in the Lau Basin and Mariana Trough.

[11] The relationship between the age of subducting oceanic lithosphere and various subduction zone parameters, including convergence rate [*Jarrard*, 1986], absolute motion of the overriding plate [*Carlson et al.*, 1983; *Jarrard*, 1986], and dip of subducting slab [*Jarrard*, 1986], has been explored using data from the present day. In their analysis only one measurement was obtained to represent an entire subduction zone for the present even though the lateral extent of these systems can be as much as 5000 km. In contrast, we have compiled the age of subducted oceanic lithosphere for each subduction zone using the most up-to-date age distribution of oceanic crust and plate reconstructions for the past 50 million years, computing the oceanic age along the strike of the trench at 100 km intervals. This results in a more complete representation of the changes in subduction-related parameters through space and time (Figures 2a–9b).

2.1. Tonga-Kermadec Trench

[12] The present-day Tonga-Kermadec subduction system is characterized by the subduction of relatively old Pacific oceanic lithosphere which formed between 85–110 Ma (Figure 2a). This crust is a remnant of spreading between the Pacific and Phoenix plates during the early-late Cretaceous [*Billen and Stock*, 2000], with the extinct spreading ridge, the Osbourn Trough, intersecting the subduction zone at latitude 26°S (Figure 2a). The youngest oceanic crust along the margin is located adjacent to the extinct spreading ridge. The present-day Tonga-Kermadec subduction zone initiated

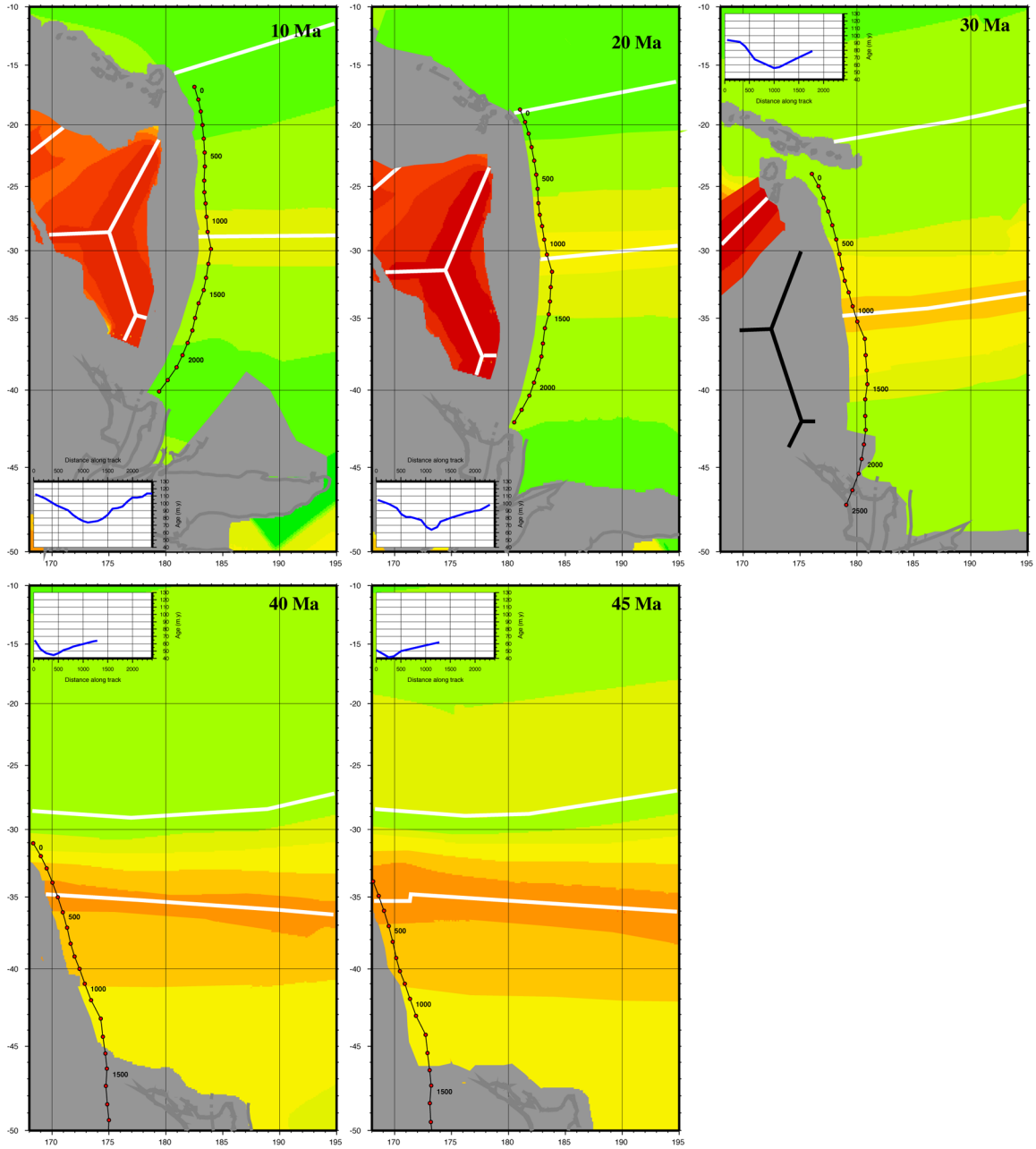

Figure 2b. Paleo-oceanic age grids of the Tonga-Kermadec system for the past 45 m.y. Scale is the same as in Figure 2. Thick black lines are active spreading ridges, and thick white lines are extinct spreading ridges.

at approximately 45 Ma [*Bloomer et al.*, 1995; *Sdrolias et al.*, 2003], during a major plate reorganization evidenced throughout the Pacific. During its inception, the margin was dominated by the subduction of 40–80 m.y. old Pacific-Phoenix crust (Figure 2b).

[13] The overriding plate is dominated by the episodic development of back-arc basins from the late Eocene to the present day. The South Fiji Basin formed between 25 and 33 Ma as two contemporaneous triple junctions [*Sdrolias et al.*, 2003] with the majority of crust forming in the northern half of the basin (Figure 2a). The initiation of the South Fiji Basin occurred when the subducting oceanic lithosphere ranged from 90 to 52 m.y. The Lau back-arc basin initiated at ~7 Ma [*Taylor et al.*, 1996; *Martinez and Taylor*, 2002] and is currently actively spreading.

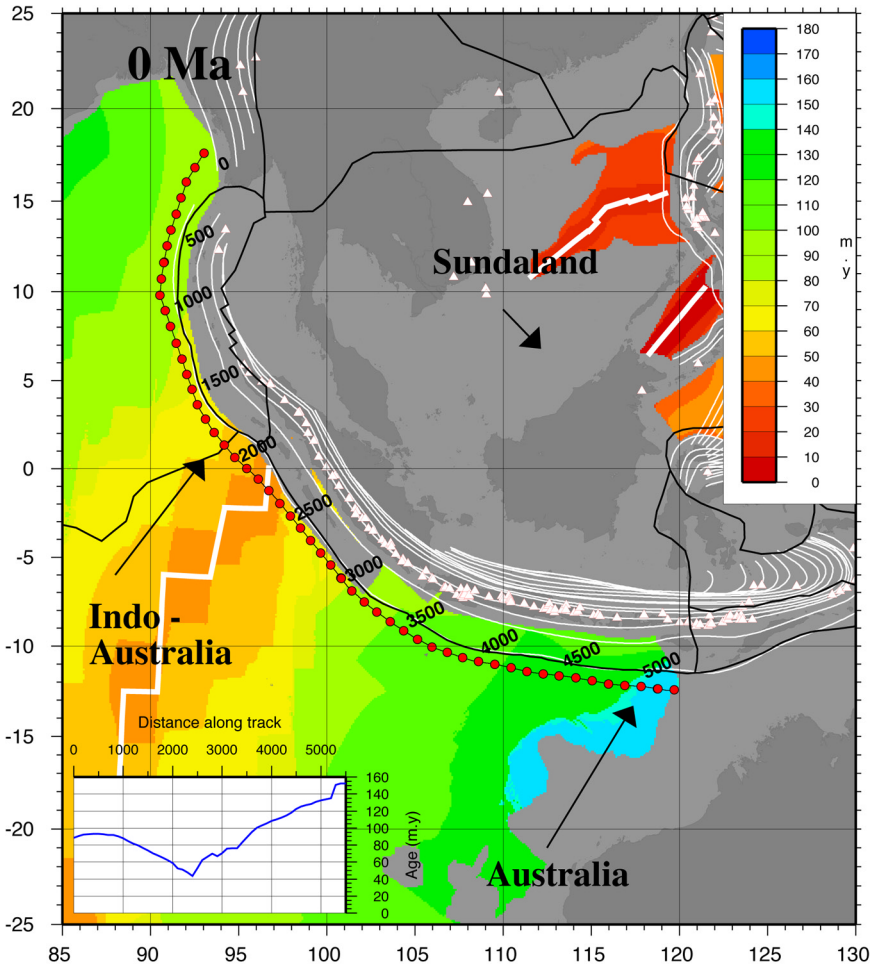

Figure 3a. Present-day age grid of the Java-Sunda subduction system. Symbols, lines, arrows, and graph are the same as in Figure 2a. Thick white lines denote the extinct Wharton Basin spreading ridge, South China Sea spreading ridge, and Sulu Sea spreading ridge.

2.2. Java-Sunda Subduction System

[14] The Java-Sunda subduction system is presently characterized by the subduction of oceanic crust which formed during several episodes of India-Australia spreading and ranges in age from 100 m.y. in the north, 43 m.y. at latitude 2°S and up to 160 m.y. in the easternmost segment of the subduction system (Figure 3a). The Java-Sunda subduction system, and its predecessor, were active back to at least the Mesozoic [*Heine et al.*, 2004] with its present configuration shaped by the extrusion of Sundaland due to the collision of India with the Eurasian plate in the late Cenozoic [*Replumaz and Tapponnier*, 2003; *Hall and Morley*, 2004].

[15] In the earliest Cenozoic, the majority of oceanic lithosphere subducted along the trench was very young (<30 m.y.), comprising crust that formed by the active Wharton Basin spreading ridge (Figure 3b). However, in the far north, remnants of 60–90 m.y. old crust, created during the early breakup between India and Australia, was actively subducted. Throughout its history, the Wharton Basin spreading ridge intersected the Java-Sunda subduction zone and this plate boundary migrated northward along the subduction zone relative to the trench. The Wharton Basin ceased spreading at approximately 43 Ma [*Liu et al.*, 1983; *Lee and Lawver*, 1995] when the age of subducted oceanic lithosphere ranged from 0 to 60 m.y. along most of the margin. Throughout its Cenozoic history, the Java-Sunda subduction system has been dominated by the subduction of very young (<40 m.y. old) oceanic lithosphere with the juxta-

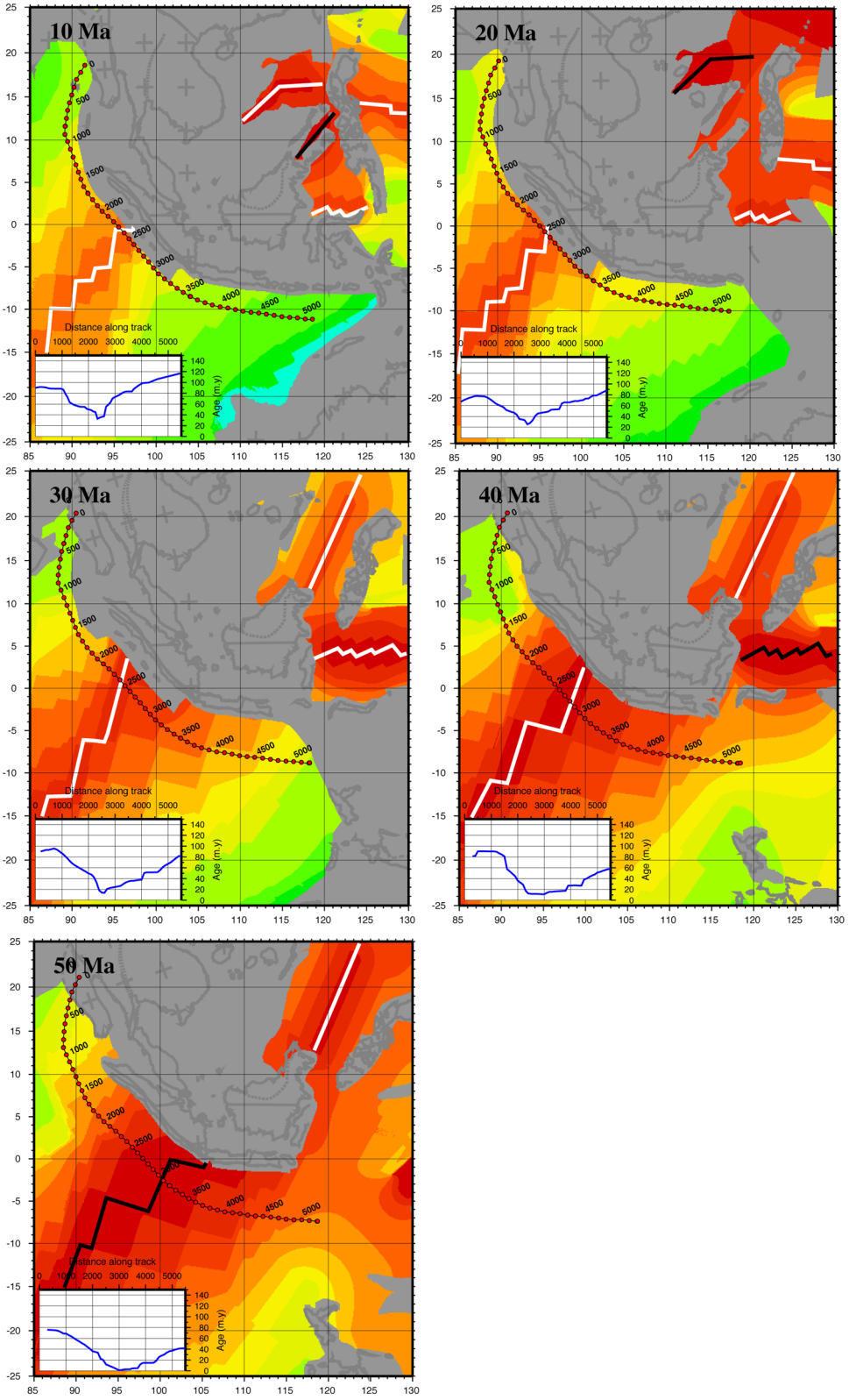

Figure 3b. Paleo-oceanic age grids of the Java-Sunda system for the past 50 m.y. Scale is the same as in Figure 3a.

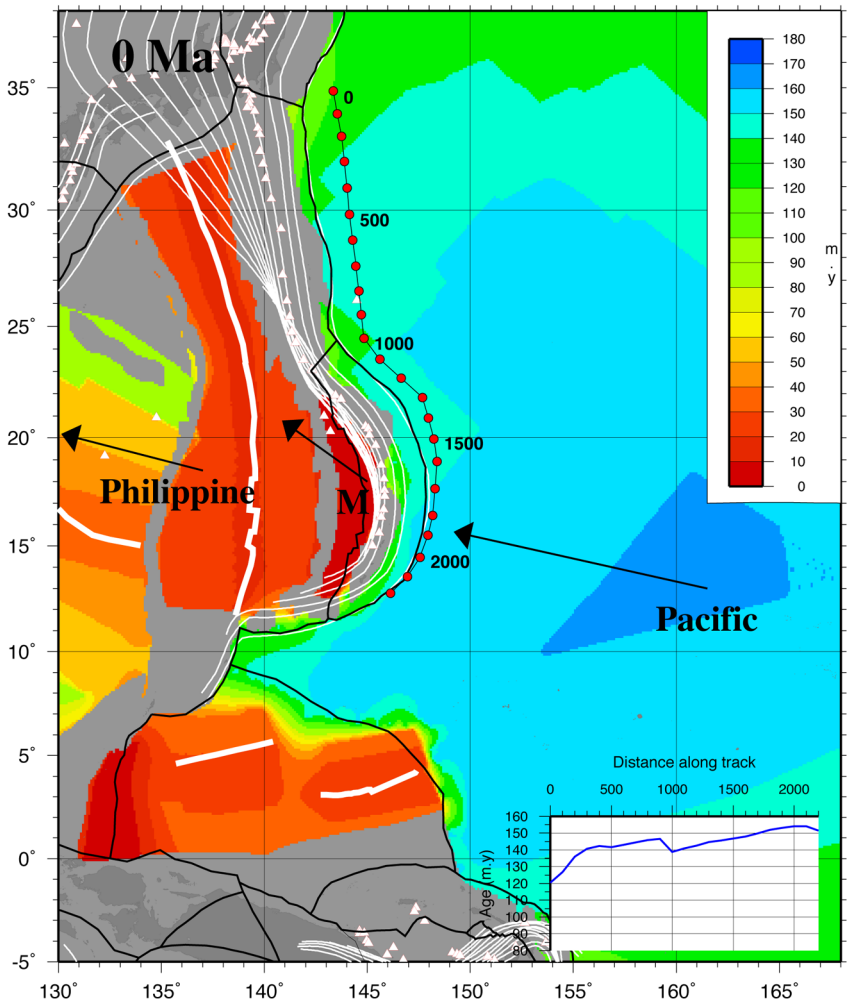

Figure 4a. Present-day age grid of the Izu-Bonin-Mariana subduction system. Symbols, lines, arrows, and graph are the same as in Figure 2a. M is Mariana Plate (Eastern Mariana Trough). Thick white lines denote the extinct plate boundaries of the West Philippine Basin, Shikoku and Parece Vela Basins, and Caroline Sea.

position of more mature crust in the far northern and far eastern segments of the subduction zone.

2.3. Izu-Bonin-Mariana Subduction System

[16] The age of the oceanic lithosphere presently subducting at the Izu-Bonin-Mariana trench is among the oldest in the world ranging from 120 to 160 m.y. and forms part of the southern flank of the extinct Pacific-Izanagi spreading system [*Nakanishi et al.*, 1989] (Figure 4a). The Izu-Bonin-Mariana subduction system initiated at about 50 m.y. [*Ben-Avraham and Uyeda*, 1983; *Stern and Bloomer*, 1992; *Hall et al.*, 2003] and has since undergone dramatic changes in its orientation, shape and location largely due to the extensive rotation of the Philippine Sea plate during the Cenozoic [*Hall et al.*, 1995]. At the time of subduction initiation, the plate boundary was oriented E-W [*Hall et al.*, 1995; *Sdrolias et al.*, 2004b] with the youngest age of subducting lithosphere being 40 m.y. and created by the Pacific-Izanagi spreading ridge (Figure 4b).

[17] The overriding plate was dominated by episodic back-arc basin formation during the Cenozoic. The West Philippine Basin formed between about 55 Ma and 30–33 Ma [*Hilde and Lee*, 1984; *Deschamps and Lallemand*, 2002]. The Parece Vela and Shikoku Basins initiated at 30 Ma [*Okino et al.*, 1998; *Sdrolias et al.*, 2004b] when the age of the subducting lithosphere ranged from 55 m.y. in the north and 100 m.y. in the south (Figure 4b). These back-arc basins ceased spreading at 15 Ma when the age of the subducting

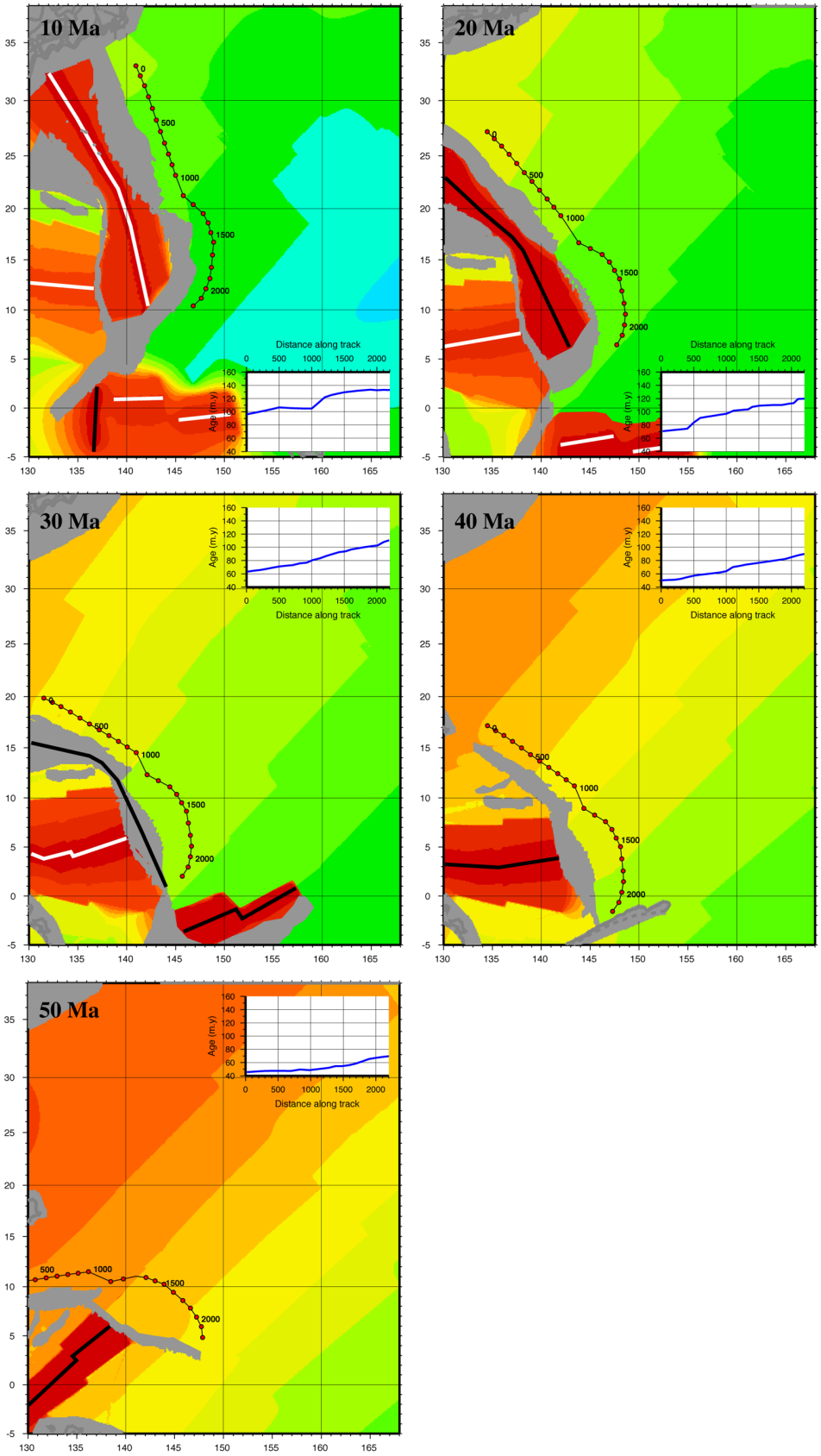

Figure 4b. Paleo-oceanic age grids of the Izu-Bonin-Mariana system for the past 50 m.y. Scale is the same as in Figure 4a.

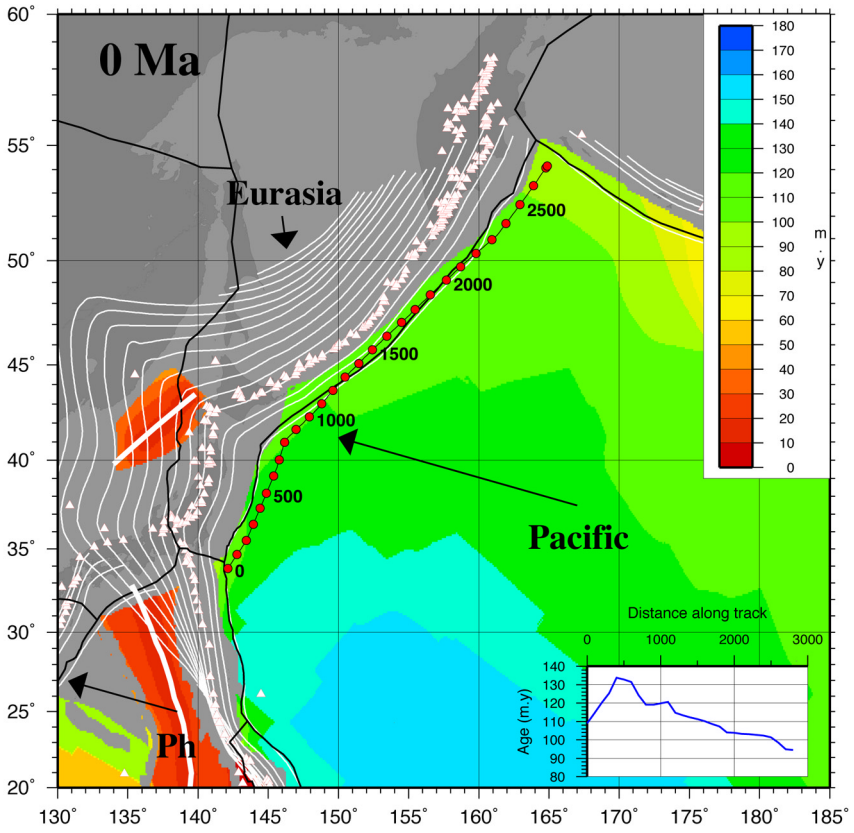

Figure 5a. Present-day age grid of the Japan-Kuril subduction system. Symbols, lines, arrows, and graph represent the same as in Figure 2a. Ph is Philippine Sea Plate. Thick white lines denote the extinct spreading ridge in the Japan Sea and Shikoku Basin.

lithosphere ranged from 90 to 125 m.y. old. Back-arc spreading resumed seaward of the Parece Vela Basin at the Mariana Trough at ~7 Ma [*Martinez et al.*, 1995] and is currently spreading.

2.4. Japan-Kuril Subduction System

[18] The Japan-Kuril subduction system is currently characterized by the subduction of old Pacific oceanic lithosphere ranging from 90 m.y. to 135 m.y. along the margin (Figure 5a). In the late Cretaceous/early Cenozoic, the Pacific-Izanagi spreading ridge was subducted subparallel to the Japan-Kuril margin (Figure 5b) and hence the age of the crust subducting along the margin dramatically increased through time to the present day.

[19] The overriding plate at the Japan-Kuril trench is the continental crust of the Eurasian plate. However, the southern margin of the Japan-Kuril trench is characterized by the formation of the Japan Sea as a back-arc basin between 15 and 30 Ma [*Jolivet et al.*, 1994]. When the Japan Sea was initiated at 30 Ma, the age of the subducting lithosphere was 60 m.y. old and the cessation of back-arc spreading occurred when the subducting crust was approximately 90 m.y. old (Figure 5b).

2.5. Aleutian Subduction System

[20] The age of subducted oceanic lithosphere at the Aleutian trench presently ranges from 100 m.y. in the west, near the juncture with the Japan-Kuril trench, to 35 m.y. in the east, south of Alaska (Figure 6a). The crust being subducted was formed by NE-SW directed Pacific-Izanagi spreading in the west [*Nakanishi et al.*, 1989], E-W Kula-Pacific spreading in the center [*Lonsdale*, 1988] and N-S Pacific-Farallon spreading [*Engebretson et al.*, 1986] in the east. In the earliest Cenozoic, the age of the crust being subducted was substantially younger than the present day, ranging from 40 to 50 m.y. along the entire margin and formed primarily from the active E-W oriented Kula-Pacific spreading ridge (Figure 6b). The Kula-Pacific spreading ceased at ~43 Ma [*Lonsdale*, 1988] and was progressively subducted along the

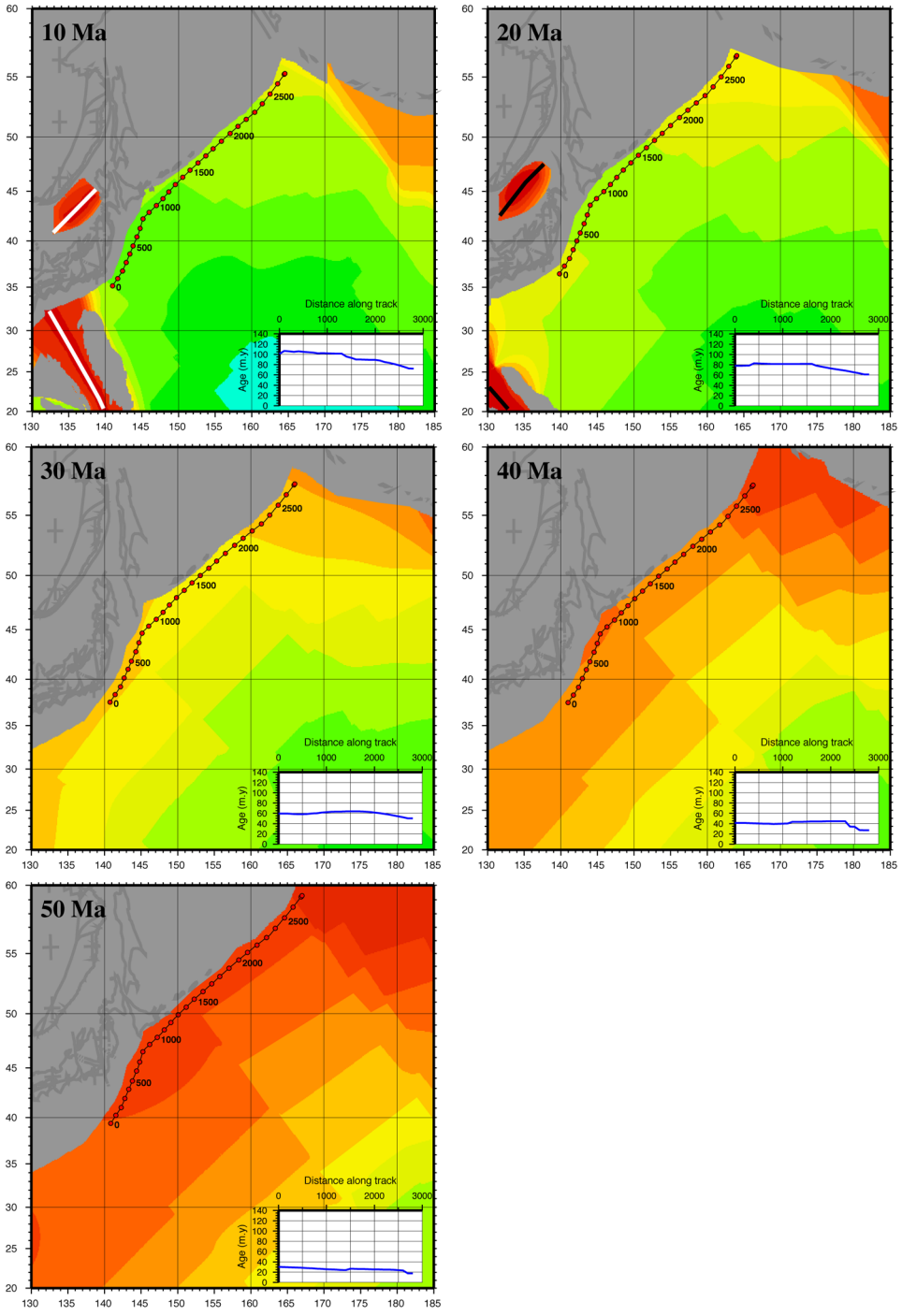

Figure 5b. Paleo-oceanic age grids of the Japan-Kuril system for the past 50 m.y. Scale is the same as in Figure 5a.

margin with subduction of the extinct spreading ridge occurring at approximately 20 Ma and was accompanied by the eruption of high Mg andesites in the central Aleutians at approximately longitude 183° [*Kelemen et al.*, 2003]. The age of the subducting oceanic lithosphere along the Aleutian margin varies along strike and with age.

2.6. Cascadia Subduction System

[21] The present-day Cascadia subduction system is characterized by the subduction of very young oceanic lithosphere of the Juan de Fuca plate [*Severinghaus and Atwater*, 1990]. The age of the crust ranges from 0 m.y. in the north where the active spreading ridge intersects the Cascadia

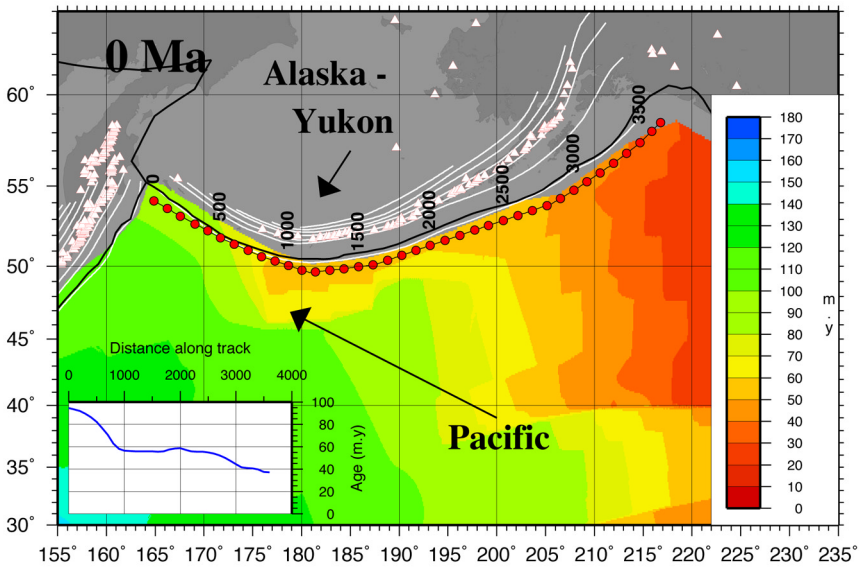

Figure 6a. Present-day age grid of the Aleutian subduction system. Symbols, lines, arrows, and graph are the same as in Figure 2a.

subduction zone, to 20 m.y. in the south where the subduction zone terminates at the Gorda fracture zone (Figure 7a). The crust at the Cascadia subduction zone remains relatively young during the entire Cenozoic and resulted in the eruption of adakitic andesites in the Mount Shasta and Lassen region of The Cascades [*Baker et al.*, 1994; *Borg et al.*, 1997] near the Mendocino triple junction. In the early Cenozoic, the crust reaches a maximum age of 40 m.y. and was formed by the northern end of the Pacific-Farallon spreading ridge. The Pacific-Farallon crust is progressively subducted at the Cascadia trench until the initiation of the Juan de Fuca ridge at 20 Ma (Figure 7b). The eastern flank of the newly created Juan de Fuca crust is subsequently subducted along the margin.

2.7. Middle America Subduction System

[22] The Middle America subduction zone is characterized by the subduction of relatively young oceanic crust that does not exceed 60 m.y. throughout its Cenozoic history. The Middle America subduction system is presently subducting the Cocos plate, the age of which varies from 0 m.y. where the active Pacific-Cocos ridge intersects the subduction zone at latitude 18° and where the active Cocos-Nazca ridge intersects the trench at latitude 7°, to 30 m.y. in the center of the Middle America subduction zone (Figure 8a). In the early Cenozoic, the age of the subducting oceanic lithosphere ranges from 25 to 60 m.y. and was formed during Pacific-Farallon spreading [*Engebretson et al.*, 1986] (Figure 8b). The Farallon plate split into the Cocos and Nazca plate at ~23 Ma. The age of the crust at the Middle America trench subsequently decreases through time as the Cocos-Nazca and Cocos-Pacific ridges and the newly formed crust from these active spreading ridges migrate toward the Middle America trench. The eruption of rocks with adakite genesis in the southern Middle America trench has been linked to the subduction of young oceanic lithosphere [*Johnston and Thorkelson*, 1997]. The age of the subducting lithosphere along the Middle America trench never exceeded 60 m.y. during the last 60 million years (Figure 8b).

2.8. Andes Subduction System

[23] The Andes subduction zone is characterized by the present-day subduction of the Nazca-Antarctic ridge at latitude 45°S in the south and of relatively young oceanic lithosphere of the Nazca plate along the central part of the margin (Figure 9a). In the far north, the age of the subducting lithosphere is less than 20 m.y. and was formed by Cocos-Nazca spreading. The present-day age of subducting oceanic lithosphere ranges from 0 m.y. at the intersection with the Nazca-Antarctic ridge, to 55 m.y. at latitude 20°S (Figure 9a). In the early Cenozoic, the age of the subducting lithosphere ranged from 30 to 60 m.y. and was formed by Pacific-Farallon spreading in the north [*Engebretson et al.*, 1986], and Farallon-

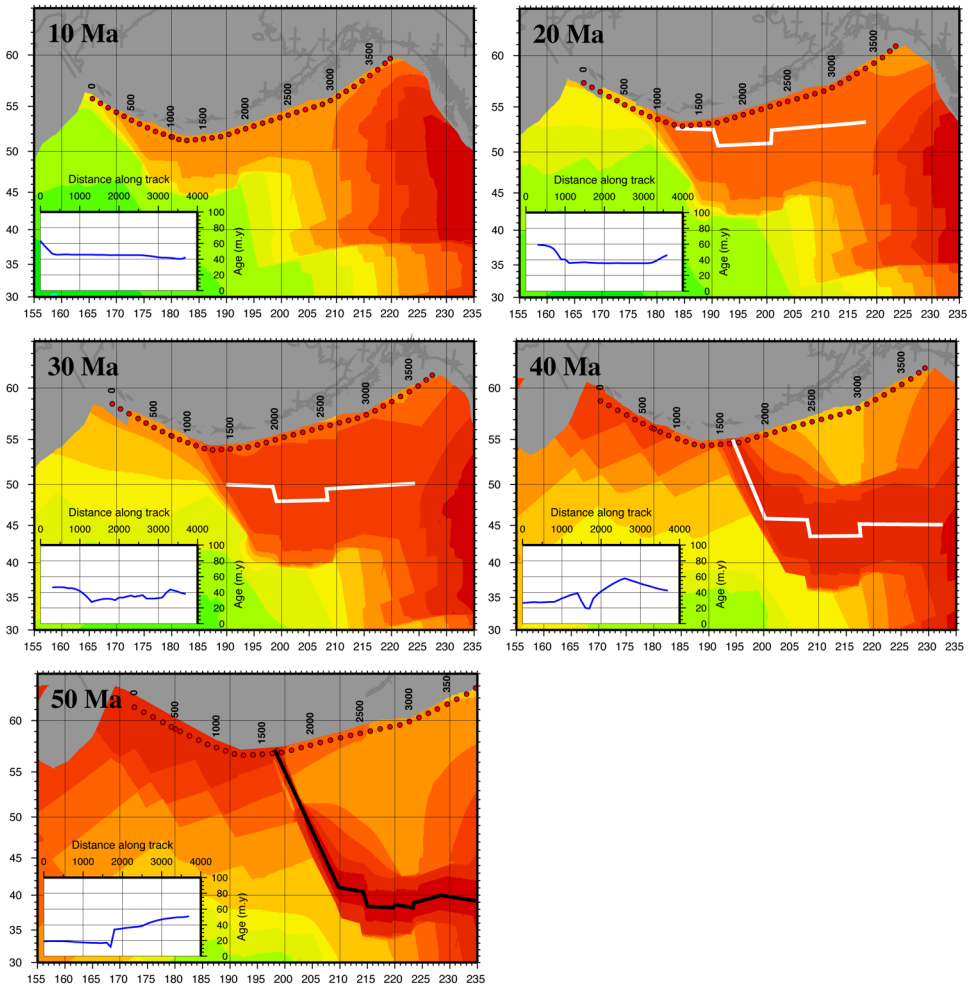

Figure 6b. Paleo-oceanic age grids of the Aleutian system for the past 50 m.y. Scale is the same as in Figure 6a.

Phoenix spreading in the center and south (Figure 9b). The Andes trench has been subject to the subduction and migration of several spreading ridges along its margin, including the Pacific-Antarctic, Pacific-Farallon and Farallon-Phoenix ridges (Figure 9b). These have significantly altered the shape, structure and dip of the subducting slab and the volcanism that has erupted on the overriding plate. The crust along the strike of the trench varies significantly through time, mainly due to its large lateral extent. However, the age of subducting lithosphere during the entire Cenozoic along this 5500 km boundary remained between 0 to 60 m.y.

2.9. Summary

[24] We group subduction zones into three distinct classes based purely on the age of subducting lithosphere: (1) Subduction zones that are currently subducting old oceanic lithosphere (>80 m.y.) along their entire length but were subducting younger oceanic lithosphere in the early Cenozoic (e.g., Tonga-Kermadec, Izu-Bonin-Mariana and Japan-Kuril trenches). (2) Subduction zones that are currently subducting young oceanic lithosphere (<40 m.y.) along their entire margin but were subducting older oceanic lithosphere in the early Cenozoic (e.g., Cascadia, Middle America and Andes subduction systems). (3) Subduction zones that are currently subducting oceanic lithosphere where the age of the crust varies substantially along strike and a similar pattern is observed during the entire Cenozoic (e.g., Aleutian and Java-Sunda trenches). The separation of the Pacific subduction zones into east and west dipping was first introduced by *Uyeda and Kanamori* [1979] and was determined by examining the present-day age of subducting lithosphere, the state of stress at the trench, the dip angle of the subducting slab and the presence/absence of back-arc basins. Our results from both the present day and the past agree with

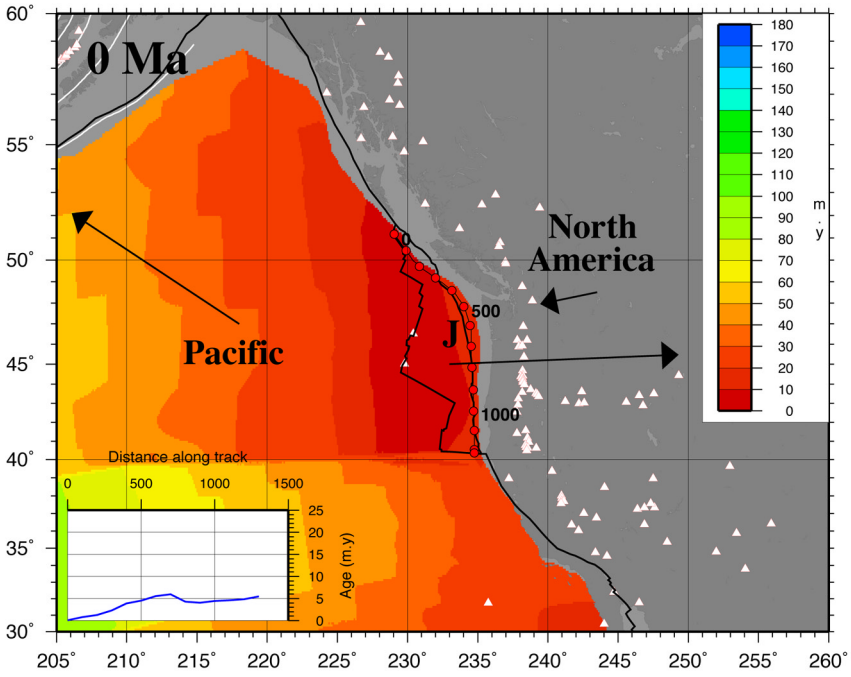

Figure 7a. Present-day age grid of the Cascadia subduction system. Symbols, lines, arrows, and graph are the same as in Figure 2a. J is Juan de Fuca Plate.

this first-order grouping of subduction zones around the Pacific. Our analysis shows that the initiation of back-arc spreading occurs in subduction zones belonging to the first group. More specifically, back-arc basins occur only when the age of the subducting oceanic lithosphere is older than about 55 m.y. and when the crust being subducted is normal oceanic lithosphere.

3. Convergence Rate and Direction

[25] The convergence rate and direction is a measure of the relative velocity between the overriding and downgoing/subducting plate and the convergence velocity is specified by the latitude, longitude and angular velocity of the pole of rotation between the two adjacent plates. As the convergence rate is a measure of the speed at which material is inserted into the mantle, it is expected that the convergence rate will have some influence on the shape, structure and behavior of the subducting slab.

[26] The convergence rate has been compared to a variety of subduction zone parameters including the age of subducting lithosphere [*Ruff and Kanamori*, 1980; *Jarrard*, 1986], the presence/absence and episodicity of backarc spreading [*Jurdy*, 1979] and the dip of the subducting slab [*Jarrard*, 1986]. Although no direct correlation was established using the convergence rate alone, studies combining the convergence rate with the age of subducting oceanic lithosphere yield important correlations between the length of the seismic zone [*Molnar et al.*, 1979], the magnitude of seismicity [*Ruff and Kanamori*, 1980] and the thermal state of the lithosphere [*Kirby et al.*, 1991].

[27] The direction of convergence indicates the degree of convergence obliquity experienced at the margin and whether shear stresses (convergence direction parallel to the margin) or normal stresses (convergence direction perpendicular to the margin) are dominant. A region with a strong shear component of subduction, such as the western Aleutians, does not have a well-defined seismic dipping zone, has limited arc volcanism on the overriding plate and no back-arc spreading is present (Figure 6a). In regions where convergence is orthogonal to the trench, such as Middle America, the margin is characterized by a prominent seismic dipping zone, steeper dipping slabs than normal and extensive arc volcanism (Figure 8a).

[28] The convergence rate and direction for each subduction system was calculated at 500 km intervals along the strike of the trench. In the regions where accurate back-arc basin spreading histories

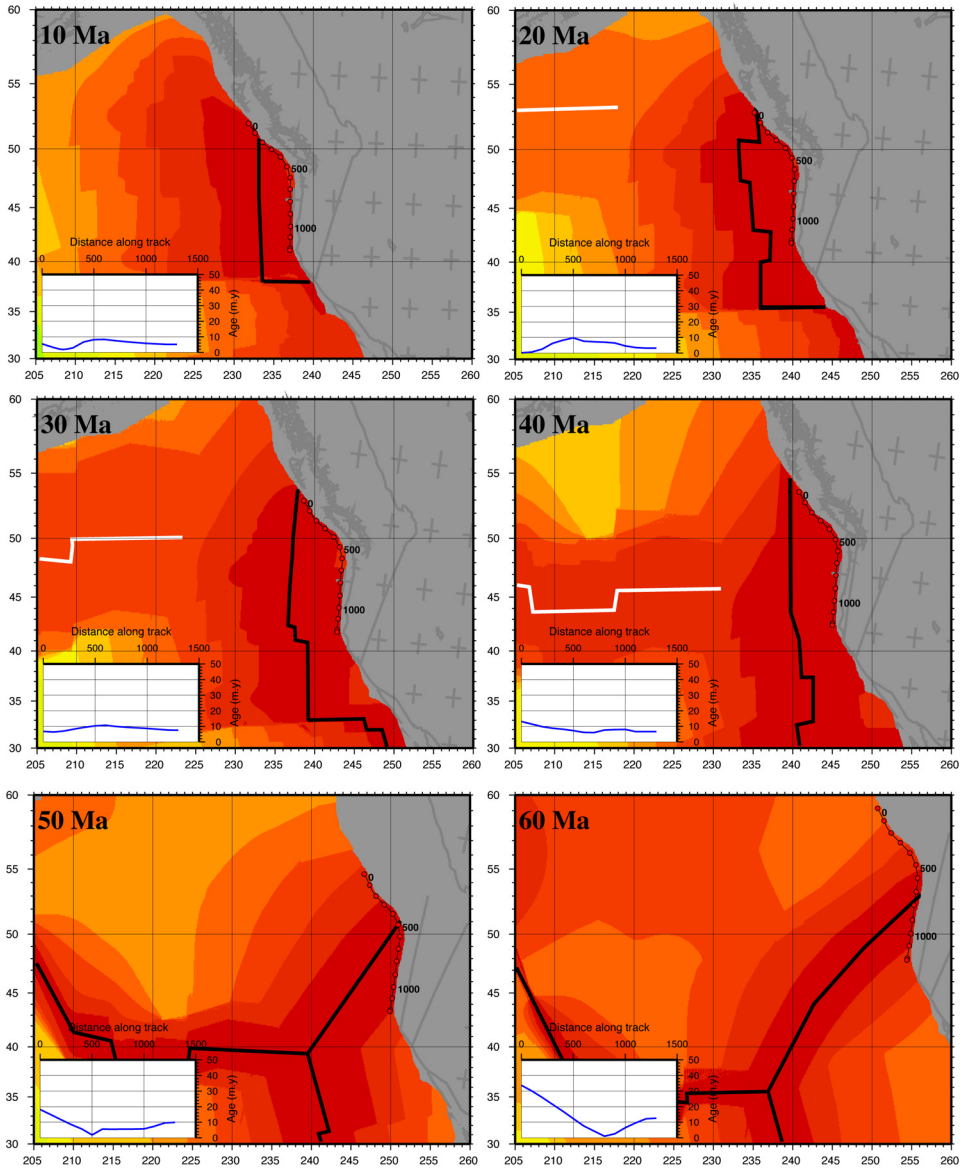

Figure 7b. Paleo-oceanic age grids of the Cascadia system for the past 60 m.y. Scale is the same as in Figure 7a.

exist (Tonga-Kermadec, Izu-Bonin-Mariana, Japan-Kuril) a separate convergence rate including back-arc basin plate was computed. We calculated the trench-normal component of convergence (i.e., the convergence rate perpendicular to the strike of the trench) as well as the trench-parallel component of convergence (Figures 10–17).

3.1. Tonga-Kermadec Subduction System

[29] The convergence rate at the Tonga-Kermadec trench was calculated by taking the Pacific plate as the downgoing plate and the Australian plate as the overriding plate during the Cenozoic. With the addition of back-arc spreading to the convergence rate the overriding Australian plate was taken to be the Australian plate from 35 to 45 Ma, the seaward South Fiji Basin plate from 25 to 35 Ma, the Australian plate from 7 to 25 Ma and the seaward Lau Basin plate from 0 to 7 Ma (Figure 10).

[30] The convergence rate in the northern half of the Tonga-Kermadec trench normal to the trench is very high (up to 130 mm/yr) including the Lau Basin (Figure 10). The incorporation of several microplates in the Lau Basin into the tectonic evolution of the basin [*Zellmer and Taylor*, 2001] may increase this convergence rate to up to 164 mm/yr and recent geodetic observations suggest the rate of convergence is as high as 240 mm/yr [*Bevis et al.*, 1995]. Even without the presence of back-arc spreading, the convergence rate would nevertheless

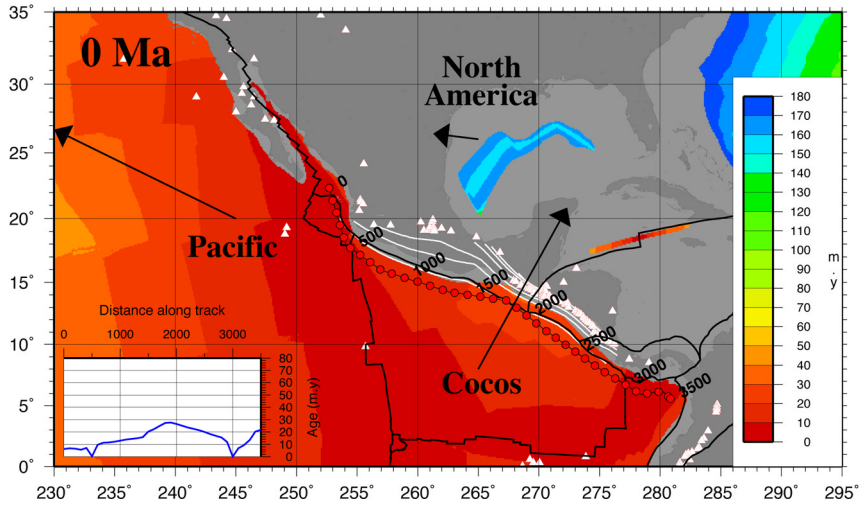

Figure 8a. Present-day age grid of the Middle America subduction system. Symbols, lines, arrows, and graph are the same as in Figure 2a.

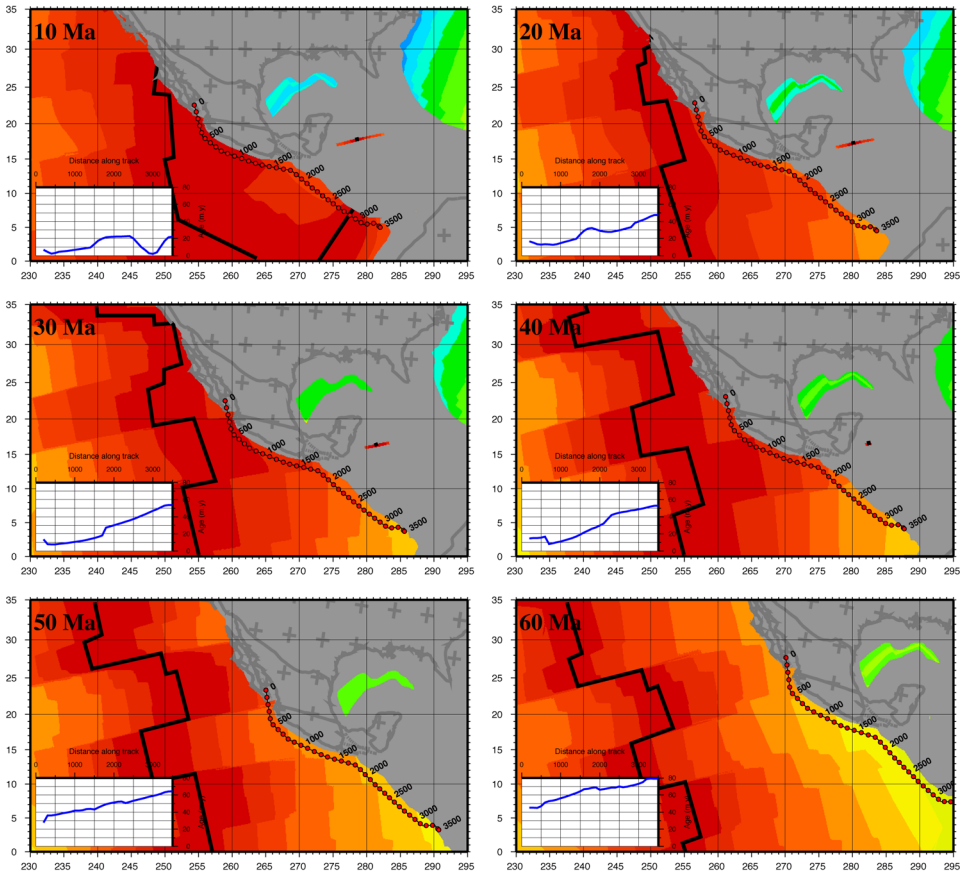

Figure 8b. Paleo-oceanic age grids of the Middle America system for the past 60 m.y. Scale is the same as in Figure 8a.

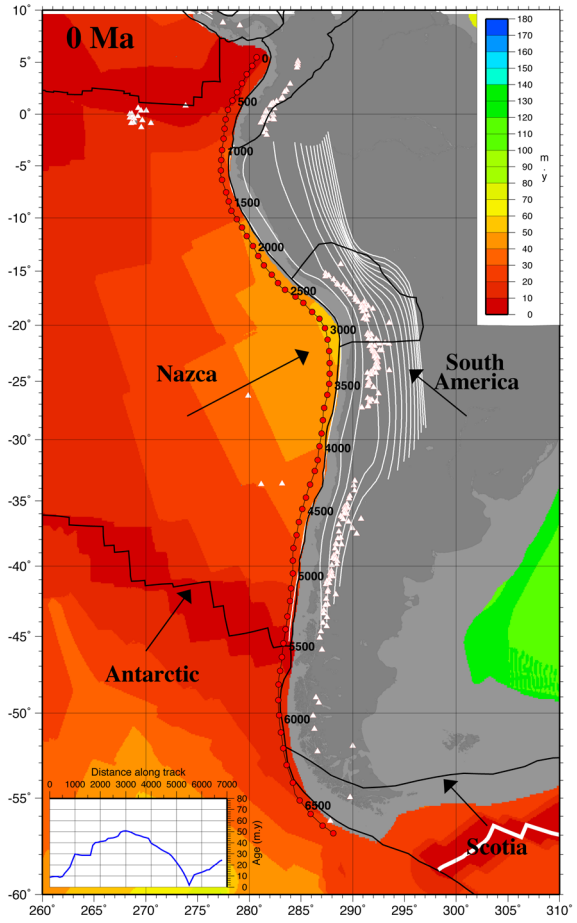

Figure 9a. Present-day age grid of the Andes subduction system. Symbols, lines, arrows, and graph represent the same as in Figure 2a.

be as high as 80 mm/yr (Figure 10) [*DeMets et al.*, 1990].

[31] The convergence rate drops to 20–60 mm/yr in the southern half of the subduction system due to the boundary effects of the position of the pole of rotation of the Australian plate to the south of Tonga-Kermadec Ridge. The convergence rate between the Pacific and Australian plate increases through time and corresponds to an increase in the age of subducting oceanic lithosphere. However, when back-arc spreading in the South Fiji Basin is initiated at ~33 Ma the convergence rate dramatically increases to up to 130 mm/yr in the trench-normal direction. The rapid spreading rate in the South Fiji Basin may be analogous to the current high spreading rates experienced in the North Fiji Basin [*Lagabrielle et al.*, 1997] and in the Lau Basin [*Taylor et al.*, 1996; *Zellmer and Taylor*, 2001]. The convergence rate prior to the initiation of back-arc basin spreading was stronger in the trench-parallel direction suggesting a significant component of shear along the boundary. However, after 35 Ma, the trench-normal component of convergence dominated the margin.

3.2. Java-Sunda Subduction System

[32] The convergence rate and direction at the Java-Sunda subduction system was calculated by taking the Australian plate as the downgoing plate from 0 to 45 Ma and the Indian plate during Wharton Basin spreading from 45 to 60 Ma north of the ridge. The overriding plate at all times was taken to be the Sumatran Block which is fixed to the Sundaland Block (Figure 3a).

[33] The Java-Sunda subduction system is noted for the great variation in the strike of the trench from the northwest to the southeast (Figure 3a) and this affects the degree of convergence obliqueness along the margin (Figure 11). In the northern Java-Sunda trench, the trench-parallel component of convergence is dominant from 0 to 30 Ma requiring oblique convergence along the northern portion of this margin. In the central Java-Sunda subduction system, the convergence rate during the Cenozoic is strongly dominated by the trench-normal component with a maximum of 120 mm/yr at 55 Ma and between 50 and 95 mm/yr between 20 and 30 Ma (Figure 11). In the eastern Java-Sunda subduction system, the orientation of the trench changes to be almost E-W (Figure 3a) and we observe strong convergence in the trench-normal direction from 0 to 30 Ma and low convergence between 30 and 60 Ma (Figure 11). We observe a sharp increase in the convergence rate after 40 Ma along the entire Java-Sunda subduction system related to the increase in spreading rate along the SE Indian Ridge and also follows from the cessation of spreading in the Wharton Basin at ~43 Ma.

3.3. Izu-Bonin-Mariana Subduction System

[34] The convergence at the Izu-Bonin-Mariana trench was calculated by taking the Pacific plate as the downgoing plate and the Philippine Sea plate as the overriding plate during the entire Cenozoic. The overriding plate, including the back-arc basin plate, is taken as the Philippine Sea plate from 30 to 50 Ma, the seaward plate of the Shikoku and Parece Vela Basins from 15 to 30 Ma, the Philippine Sea plate from 7 to 15 Ma and the seaward plate of the Mariana Trough from 0 to 7 Ma (Figure 12).

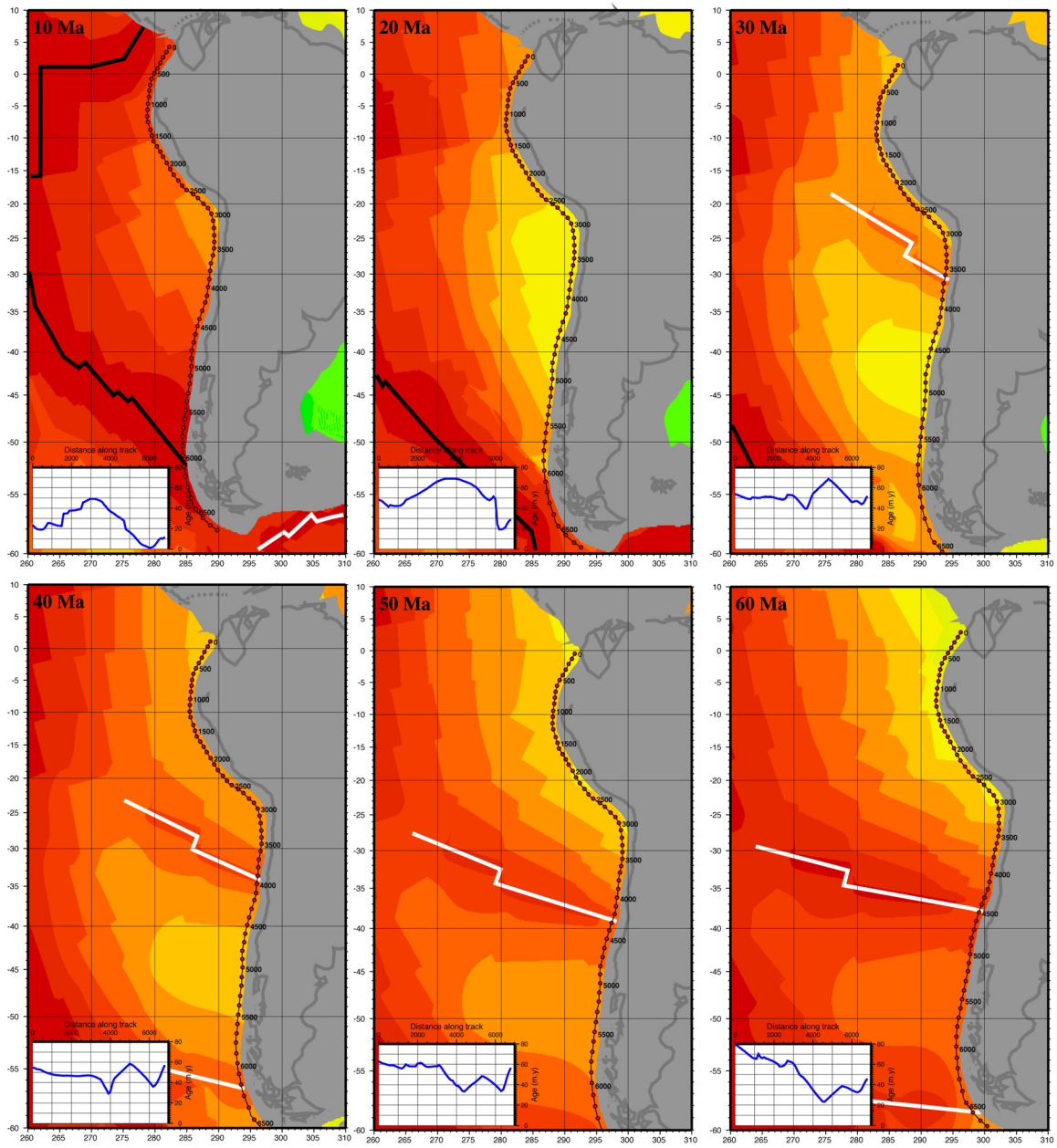

Figure 9b. Paleo-oceanic age grids of the Andes system for the past 60 m.y. Scale is the same as in Figure 9a.

[35] In our model, the convergence rate during subduction initiation was extremely high, peaking at 340 mm/yr in the early Cenozoic and corresponding to the large clockwise rotation and westward translation of the Philippine Sea plate relative to the Pacific plate [*Hall et al.*, 1995]. There is a sharp decrease in the convergence rate to between 10 and 50 mm/yr after 40 Ma (Figure 12) and this is related to the cessation of rotation of the Philippine Sea plate and changing orientation of the plate boundary. The initiation of back-arc spreading in the Parece Vela and Shikoku Basins at 30 Ma [*Sdrolias et al.*, 2004b] corresponds to a period where the parallel component of convergence is greater than the normal component and the trench-normal component does not exceed 30 mm/yr. However, when the back-arc basin plate is included into the overriding plate motion, the convergence rate has a higher trench-normal than trench-parallel component with an increased convergence rate during back-arc spreading. The cessation of back-arc spreading at 15 Ma corresponds to a decrease in the convergence rate (including the back-arc plate) but an increase in the convergence between the

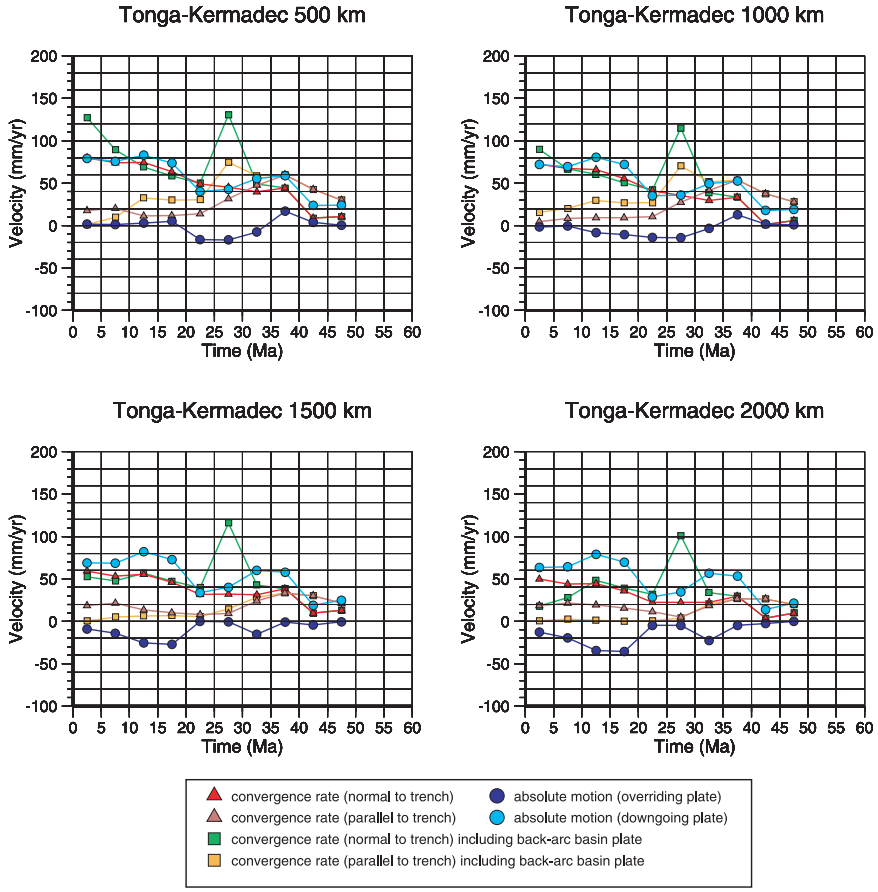

Figure 10. A series of graphs representing velocity data from the Tonga-Kermadec subduction system for the (top left) 500 km, (top right) 1000 km, (bottom left) 1500 km and (bottom right) 2000 km point marks (see Figure 2a for location of points). These results are plotted over time for the past 50 million years, and each point represents the midpoint of 5 million year tectonic stages. Positive values mean motion is toward the trench. Negative values mean motion is away from the trench.

Pacific and Philippine Sea plate. This can be attributed to the commencement of clockwise rotation of the Philippine Sea plate at 20–21 Ma [*Sdrolias et al.*, 2004b]. The initiation of back-arc spreading in the Mariana Trough at 7 Ma is accompanied by an increase in convergence rate but decreases to 60 mm/yr maximum after an increase in the rotation of the Philippine Sea plate at 5 Ma. The rotational history of the Philippine Sea plate [*Hall et al.*, 1995] has strongly influenced the convergence history of the Izu-Bonin-Mariana subduction system and may explain why there is an inverse relationship between the age of the subducting lithosphere and the magnitude of convergence (Figure 12).

3.4. Japan-Kuril Subduction System

[36] The convergence rate and direction for the Japan-Kuril subduction system was calculated by taking the Pacific plate as the downgoing plate and the Eurasian plate as the overriding plate during the Cenozoic (Figure 13). When the back-arc basin plate of the Japan Sea was incorporated into the motion of the overriding plate, the overriding plate was taken as the Eurasian plate from 30 to 50 Ma, the seaward side of the Japan Sea from 15 to 30 Ma and the Eurasian plate from 0 to 15 Ma.

[37] The convergence rate along the Japan-Kuril subduction zone increases from north to south during the Cenozoic. Throughout the Cenozoic, the Japan-Kuril margin is dominated by a strong trench-normal component of convergence, ranging from 100 mm/yr at the present-day in the south to 80 mm/yr in north. An increase in the convergence rate occurs between 40 and 45 Ma along the entire margin and may be related to the change in spreading direction in the Pacific. The initiation of spreading in the Japan Sea at 30 Ma corresponds to a convergence rate of between 60 and 80 mm/yr

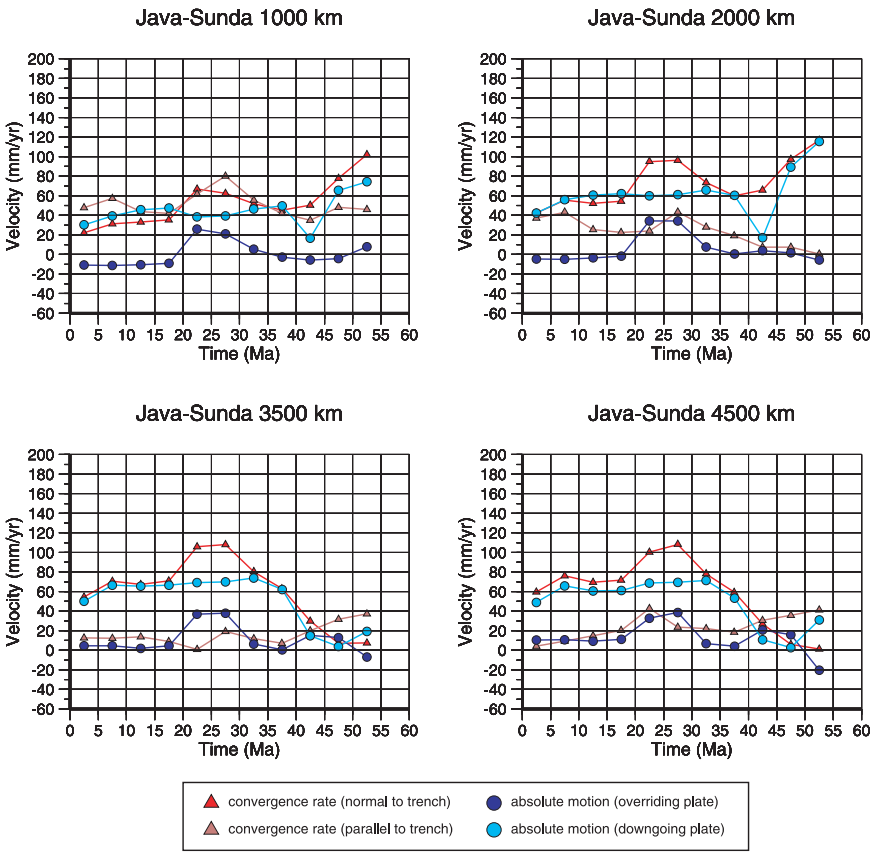

Figure 11. A series of graphs representing data from the Java-Sunda subduction system for the (top left) 1000 km, (top right) 2000 km, (bottom left) 3500 km, and (bottom right) 4500 km point marks (see Figure 3a for location of points). See Figure 10 for description of graphs.

and its cessation at 15 Ma is marked by a decrease in total convergence rate (including the back-arc plate) but an increase in the convergence between the Pacific and Eurasian plates.

3.5. Aleutian Subduction System

[38] The convergence rate and direction values for the Aleutian subduction system were calculated by taking the Kula plate as the downgoing plate from 30 to 60 Ma and the Pacific plate from 0 to 30 Ma. The overriding plate was taken to be the Alaska-Yukon plate which is fixed to the North American plate during the Cenozoic (Figure 14).

[39] The orientation of the Aleutian subduction system varies greatly along strike and thus significantly affects the convergence history along the margin. In the western Aleutians, little to no convergence is occurring and the margin is dominated by strike-slip motion (Figure 14). The lack of active volcanism in this portion of the Aleutian island arc chain and the lack of a dipping zone of seismicity (Figure 6a) supports the absence of a trench-normal component of convergence in this region. In the central and eastern sections of the Aleutian trench (Figure 14), the convergence rate reaches values greater than 100 mm/yr between 35 and 55 Ma, but this steadily decreases through time until 15 Ma. After 15 Ma and the subduction of the Kula-Pacific ridge, the convergence rate increases from 40 to 70 mm/yr.

3.6. Cascadia Subduction System

[40] The convergence rate and direction data for the Cascadia subduction system were calculated by taking the Farallon plate as the downgoing plate between 20 and 60 Ma and the Juan de Fuca plate from 0 to 20 Ma. The overriding plate is taken to be the North American plate during the entire Cenozoic.

[41] The convergence rate normal to the trench at the Cascadia subduction zone is quite high throughout most of the Cenozoic, reaching a maximum value of 155 mm/yr in the trench-normal

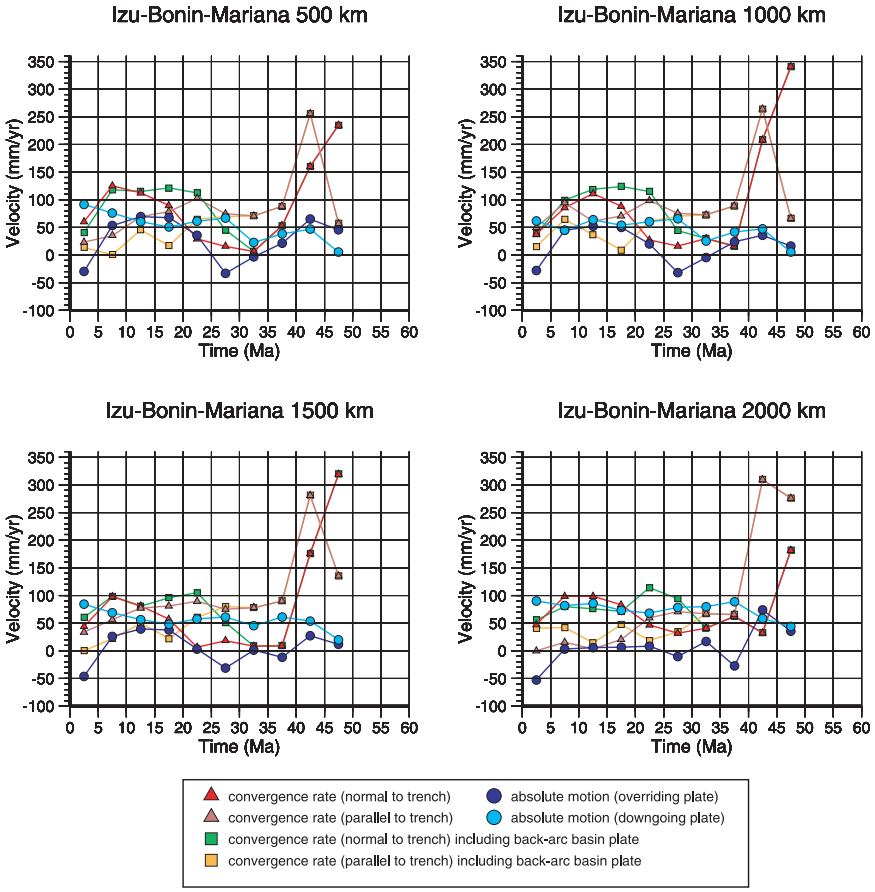

Figure 12. A series of graphs representing data from the Izu-Bonin-Mariana subduction system for the (top left) 500 km, (top right) 1000 km, (bottom left) 1500 km, and (bottom right) 2000 km point marks (see Figure 4a for location of these points). See Figure 10 for description of graphs.

direction between 50 and 55 Ma (Figure 15) during Pacific-Farallon spreading. The convergence rate steadily decreases to 65 mm/yr until 20 Ma. The creation of the Juan de Fuca plate at 20 Ma is followed by a decrease in the convergence rate and a change from trench-normal to dominant trench-parallel convergence between 10 and 20 Ma. The convergence rate between 0 and 10 Ma is dominated by trench-normal convergence and the convergence rate increases from 40 to 110 mm/yr.

3.7. Middle America Subduction System

[42] The convergence data for the Middle America subduction system were calculated based upon the Farallon plate as the downgoing plate between 23 and 60 Ma and the Cocos plate from 0 to 23 Ma. The overriding plate was taken to be the Caribbean plate which we have fixed to the North American plate during the Cenozoic (Figure 16).

[43] The trench-normal component of convergence at the Middle America trench varies along the strike of the trench, principally due to the change in the shape of the subduction zone along the margin. The present-day trench-normal component of convergence increases southward along the margin, from 20 mm/yr in the north to 105 mm/yr in the south due to the different plates subducting along the margin at this time. The fastest convergence rates are experienced in the early Cenozoic associated with the subduction of Pacific-Farallon crust when the convergence rate reaches a maximum of 185 mm/yr in the north and 160 mm/yr in the south (Figure 16). The southern Middle America trench experienced a sharp increase in convergence rate at 20 Ma and may be related to the breakup of the Farallon plate into the Cocos and Nazca plates. In the northern Middle America trench, a sharp decrease in the convergence rate was experienced at 10 Ma.

3.8. Andes Subduction System

[44] The convergence rate and direction data for the Andes subduction system were calculated by taking the Nazca plate as the downgoing plate

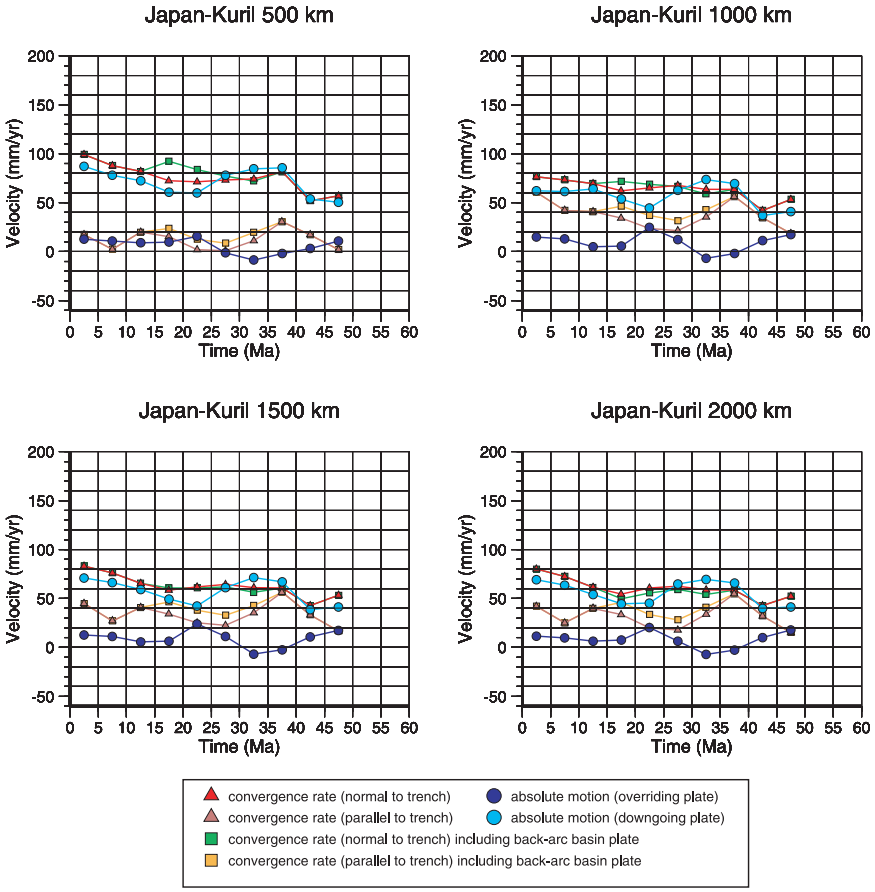

Figure 13. A series of graphs representing data from the Japan-Kuril subduction system for the (top left) 500 km, (top right) 1000 km, (bottom left) 1500 km, and (bottom right) 2000 km point marks (see Figure 5a for location of these points). See Figure 10 for description of graphs.

between 0 and 23 Ma north of latitude 45°S and the Farallon plate from 23 to 60 Ma north of latitude 45°S. The downgoing plate was taken to be the Antarctic plate south of latitude 45°S. The overriding plate was taken to be the South American plate during the entire Cenozoic (Figure 17).

[45] The Andes subduction system is dominated by very high rates of convergence in the northern and central portions of the margin and has been dominated by the trench-normal component of subduction throughout the entire Cenozoic. The present-day convergence rate ranges from 50 mm/yr in the north, 65 mm/yr in the central and 20 mm/yr in the far south of the margin (Figure 17). The present-day constitutes the slowest convergence rate along the Andes for at least the past 60 m.y. The convergence rate reaches a maximum velocity of 160 mm/yr between 50 and 55 Ma in the northern part of the Andes trench (Figure 17). The trench-parallel component of convergence is small but steadily increases southward. There is a sharp increase in the convergence rate between 50 and 55 Ma and this lasts until 45 Ma, after which there is a decrease in convergence rate.

[46] The breakup of the Farallon plate into the Cocos-Nazca plate at 23 Ma caused a slight increase in the convergence rates along the margin. The character of convergence changes remarkably south of 45°S to be small in magnitude due to the motion of the downgoing plate (the Antarctic plate in this region).

3.9. Summary

[47] The convergence history along each of our studied subduction zones reveals that the trench-normal component of convergence is almost always dominant with rates generally ranging from 30 mm/yr to 100 mm/yr. Major peaks in convergence rate are experienced at the Izu-Bonin-Mariana trench during the large clockwise rotation of the overriding plate and also during the early-mid Eocene (40–55 Ma) along the eastern Pacific

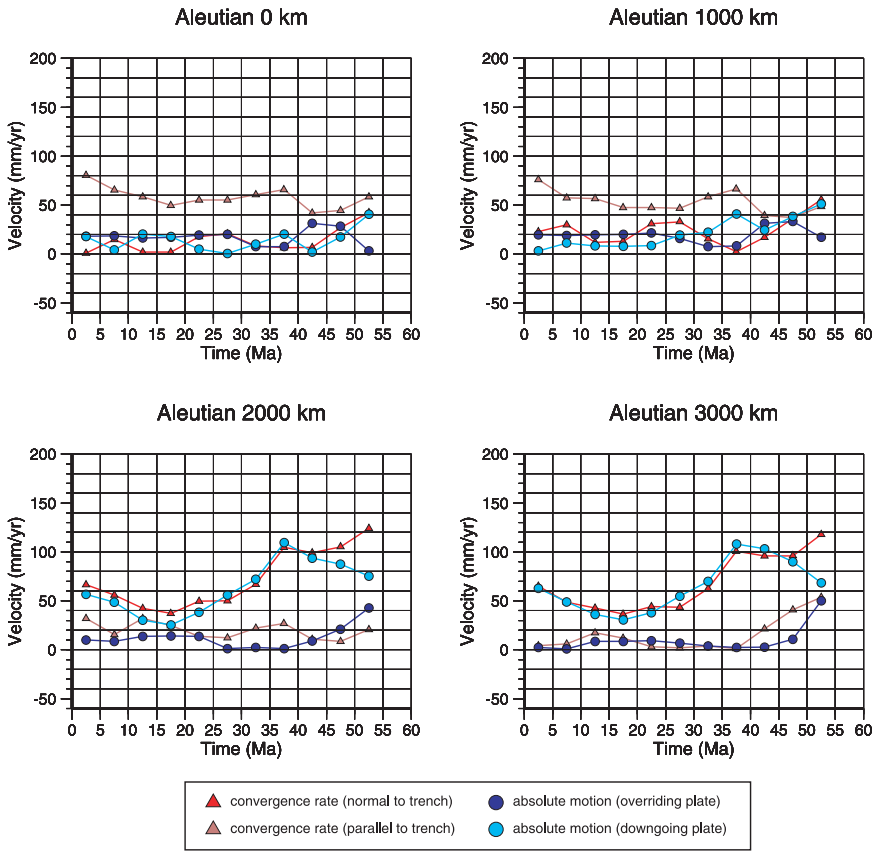

Figure 14. A series of graphs representing data from the Aleutian subduction system for the (top left) 0 km, (top right) 1000 km, (bottom left) 2000 km, and (bottom right) 3000 km point marks (see Figure 6a for location of these points). See Figure 10 for description of graphs.

margin. Small trench-normal convergence rates, with a large component of shear are experienced in the western Aleutians and the southern Andes margin. In the Western Pacific, we observe an increase in the convergence rate while back-arc spreading is active and is directly attributed to the seaward motion of the back-arc basin plate during seafloor spreading.

4. Absolute Motion of the Downgoing and Overriding Plates

[48] The absolute motion of a plate is a measure of the velocity of an individual plate relative to the spin axis of the Earth. The absolute reference frame which best approximates the motion of individual plates is a controversial issue but has previously been based, most commonly, on the fixed hot spot reference frame [e.g., *Müller et al.*, 1993]. In this study we have used a new absolute reference frame based on Atlantic-Indian moving hot spots [*O'Neill et al.*, 2005] as we believe it best approximates an absolute reference frame at least for the past 80 m.y. In studies of subduction and back-arc basin dynamics, the absolute motion of the downgoing and overriding plates, is an important constraint on determining the migration and rollback history of the subduction hinge,, the amount of strain on the overriding plate and the manifestation of this strain on the surface of the overriding plate.

[49] A relationship between the age of the subducting lithosphere and the absolute rate of motion of the subducting plate was established by *Carlson et al.* [1983] and *Carlson and Herrick* [1990] and has implications for models of slab pull. More significant for back-arc basin studies is the absolute motion of the overriding plate which has been confirmed by present-day observations [*Heuret and Lallemand*, 2005; *Lallemand et al.*, 2005]. Previous studies have suggested that the direction of absolute motion of the overriding plate determines whether back-arc spreading develops on the overriding plate [*Chase*, 1978; *Uyeda and Kanamori*, 1979; *Scholz and Campos*, 1995]. The motion of the overriding plate toward the trench in an absolute sense results in seismic coupling at the

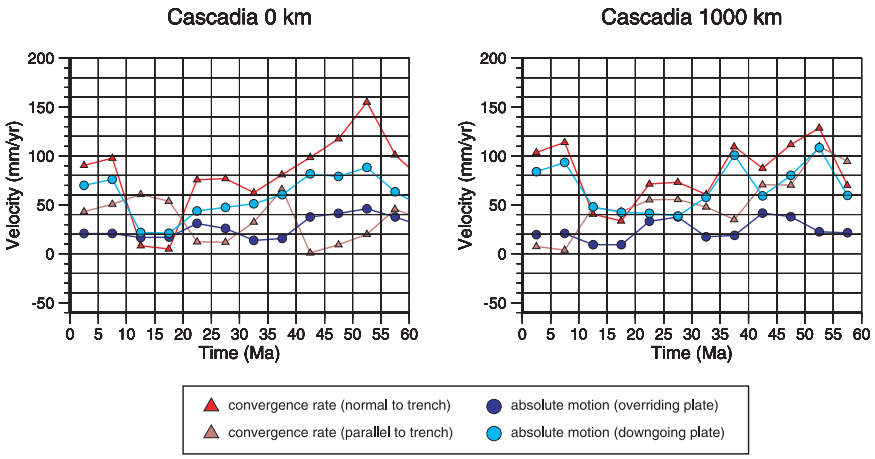

Figure 15. A series of graphs representing data from the Cascadia subduction system for the (left) 0 km and (right) 1000 km point marks (see Figure 7a for location of these points). See Figure 10 for description of graphs.

trench, a compressional state of stress on the overriding plate and no back-arc extension. The motion of the overriding plate away from the trench in an absolute sense, results in seismic decoupling at the trench, an extensional state of stress on the overriding plate and the development of back-arc spreading.

[50] We have computed the absolute motion for both the downgoing/subducting and overriding

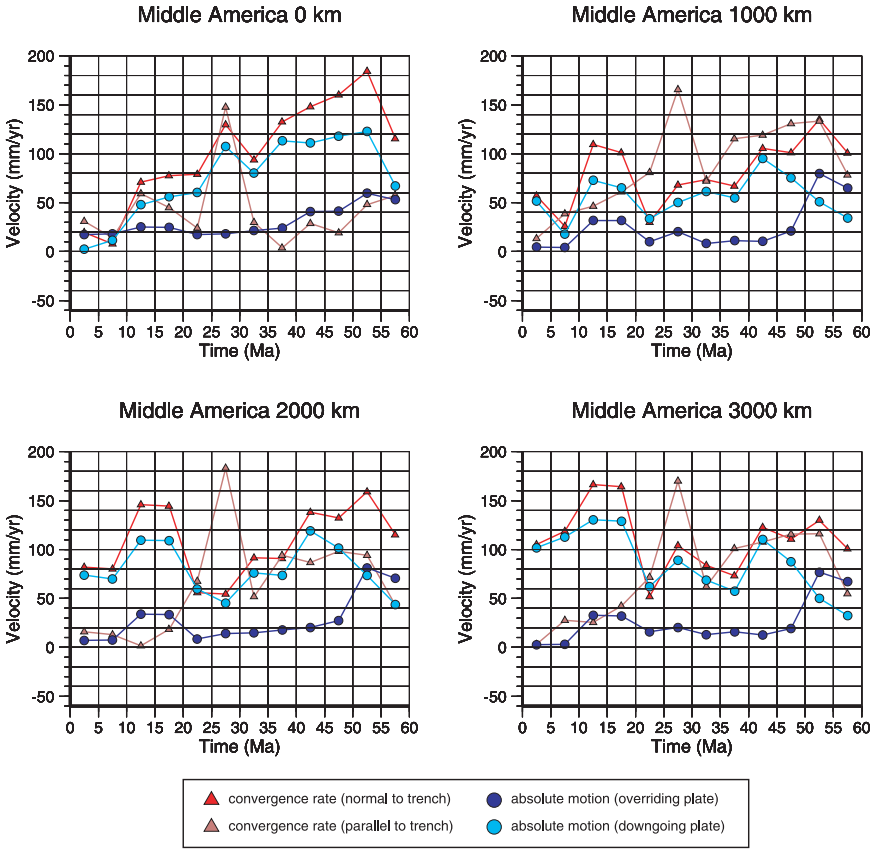

Figure 16. A series of graphs representing data from the Middle America subduction system for the (top left) 0 km, (top right) 1000 km, (bottom left) 2000 km, and (bottom right) 3000 km point marks (see Figure 8a for location of these points). See Figure 10 for description of graphs.

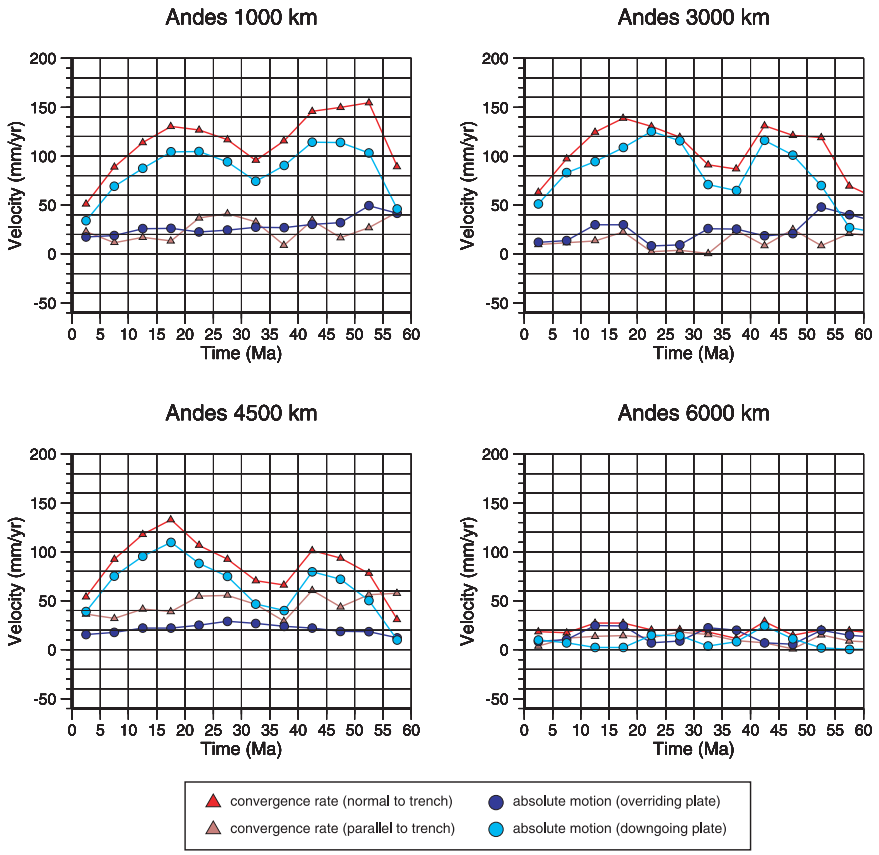

Figure 17. A series of graphs representing data from the Andes subduction system for the (top left) 1000 km, (top right) 3000 km, (bottom left) 4500 km, and (bottom right) 6000 km point marks (see Figure 9a for location of these points). See Figure 10 for description of graphs.

plates at each subduction zone for every 500 km interval along the strike of the trench (Figures 10–17). The absolute motion of the downgoing and overriding plate is calculated as the trench-normal component of motion.

4.1. Tonga-Kermadec Subduction System

[51] The subducting Pacific plate at the Tonga-Kermadec margin possesses a strong component of motion toward the trench with increasing velocities to the north. Initially, the Pacific plate was moving toward the trench at approximately 20 mm/yr with a sharp increase after 40 Ma to an average of 60 mm/yr (Figure 10). The Pacific plate is currently moving toward the Tonga-Kermadec trench at an average 70 mm/yr normal to the trench.

[52] The overriding Australian plate, in contrast, has had a small component of trench-normal motion along the strike of the trench throughout its history. In the northern Tonga-Kermadec trench, the overriding plate was moving toward the trench at up to 18 mm/yr between 35 and 50 Ma. Thereafter, the absolute motion of the overriding plate changed such that the Australian plate moved slightly away from the trench until 20 Ma in the far north and 10 Ma in the center. The beginning of the landward migration of the overriding plate corresponds both to the initiation of back-arc spreading in the South Fiji Basin at 33 Ma and a period of decline in the magnitude of motion of both the downgoing and overriding plates. As back-arc spreading developed in the South Fiji Basin, the magnitude of this motion became more pronounced in the north than the south where the basin is widest. The motion of the overriding plate away from the trench continued throughout the history of South Fiji Basin spreading and until 20 Ma in the far north of the margin. The overriding plate subsequently moved toward the trench between 10 and 20 Ma. The initiation of spreading in the Lau Basin at ~7 Ma again corresponds to the absolute motion of the overriding plate away from the trench or with little motion of the overriding plate in either direction (Figure 10). The Australian plate has been moving away (land-

ward) from the trench from 0 to 45 Ma in the southern portion of the margin (Figure 10).

4.2. Java-Sunda Subduction System

[53] The absolute motion of the downgoing plate normal to the trench along the Java-Sunda margin varies along strike but with increasing motion toward the southeast. We observe a sharp decline in the motion of the downgoing plate between 40 and 45 Ma corresponding to the cessation of spreading in the Wharton Basin at ~43 Ma, and a sharp increase in the motion of the downgoing plate after 40 Ma related to the increase in spreading rate along the SE Indian Ridge [*Heine et al.*, 2004] (Figure 11). The fastest velocity of the downgoing plate toward the trench occurred in the early Cenozoic.

[54] The absolute motion of the overriding plate has a similar pattern along the strike of the trench, except in the southeast where the orientation of the trench strikes E-W. The overriding plate was moving slowly toward the trench between 20 and 40 Ma in the north and 20 and 50 Ma in the center of the margin of between 1 and 30 mm/yr. Thereafter, the overriding plate was moving away from the trench at a similar velocity. The Andaman Sea formed oceanic crust during the Miocene to the present, at the time when the overriding plate was moving away form the trench in this location. However, this basin is believed to be controlled by strike-slip motions associated with the collision of India and Eurasia [*Chamot-Rooke et al.*, 2001], rather than the rollback of the subduction hinge. In the southeastern portion of the margin, the overriding plate moves toward the trench throughout most of the Cenozoic. It is important to note that our profile does not extend to the region adjacent to the Banda Sea back-arc region.

4.3. Izu-Bonin-Mariana Subduction System

[55] The absolute motion of the overriding plate (Philippine Sea plate) and the orientation and location of the Izu-Bonin-Mariana trench through time is constrained by paleomagnetic studies of the Philippine Sea plate [*Hall et al.*, 1995]. Paleomagnetic studies have been used to determine the rotation of the Philippine Sea plate as its motion through time cannot be linked to the global plate circuit due to the Philippine Sea plate being entirely surrounded by subduction zones.

[56] The absolute motion of the downgoing plate along the Izu-Bonin-Mariana trench steadily increases through time and appears to be related to the dramatic change in orientation of the trench during its clockwise rotation rather than changes in the spreading history of the downgoing Pacific plate. In the early Cenozoic, the absolute motion of the downgoing plate ranged from 10 to 60 mm/yr (Figure 12), The present-day velocity of the downgoing plate ranges from 90 mm/yr in the north and center and 80–90 mm/yr in the southern end of the margin.

[57] The absolute motion of the overriding plate in the northern Izu-Bonin-Mariana trench was toward the trench between 30 and 50 Ma with velocities ranging from 0 to 60 mm/yr (Figure 12) simultaneous with spreading in the West Philippine Basin. At 30 Ma, the absolute motion of the overriding plate changed from toward the trench to away from the trench and corresponds to the initiation of back-arc spreading in the Parece Vela and Shikoku Basins [*Sdrolias et al.*, 2004b]. In the south, the absolute motion of the overriding plate changes from toward the trench to away form the trench at 35 Ma (Figure 12). The overriding plate continues to migrate away from the trench until 20–25 Ma, corresponding to the onset of clockwise rotation of the Philippine Sea plate. The overriding plate moves away from the trench during the opening of the Mariana Trough due to the initiation of rotation of the Philippine Sea plate at 5 Ma [*Hall et al.*, 1995].

4.4. Japan-Kuril Subduction System

[58] The absolute motion of the downgoing plate at the Japan-Kuril subduction system increased through time from north to south peaking at 85 mm/yr between 35 and 40 Ma in the south (Figure 13). The absolute motion of the downgoing Pacific plate increases steadily after 15 Ma and is presently 85 mm/yr in the south. The velocities of the downgoing plate are high compared with the velocity values for the overriding plate. The increase in velocity of the Pacific plate southward is a function of the location of the pole of rotation of the Pacific plate with respect to the position of the trench.

[59] The absolute motion of the overriding plate along the Japan-Kuril trench never exceeds 20 mm/yr along the entire margin (Figures 13a and 13b). The overriding plate travels toward the trench between 40 and 60 Ma and then migrates slowly away from the trench between 25 and 40 Ma. After 25 Ma, the overriding plate again travels

toward the trench but with a greater velocity. The initiation of spreading in the Japan Sea occurred at 30 Ma [*Jolivet et al.*, 1994] corresponding to the period when the overriding plate was migrating away from the trench. During the development of the Japan Sea, the overriding plate was migrating away from the trench until 25 Ma and was traveling toward the trench when back-arc spreading in the Japan Sea discontinued.

4.5. Aleutian Subduction System

[60] The Aleutian subduction system can be separated into two groups: a western and central-eastern section based on the orientation of the trench. In the western Aleutians, the absolute motion of both the downgoing and overriding plate is quite small (Figure 14). However, the overriding plate migrates toward the trench with a faster velocity than the downgoing plate during the Oligocene-Miocene. The plate boundary in this region is predominately strike-slip.

[61] In the central and eastern section of the Aleutian trench, the character of the trench-normal component of velocity of the downgoing and overriding plates change markedly compared to the western portion. The downgoing plate has a fast velocity toward the trench, up to 110 mm/yr between 35 and 50 Ma throughout its history (Figure 14). Thereafter, the downgoing plate decreases in velocity to 30 mm/yr between 15 and 20 Ma and then subsequently increases to be about 60 mm/yr at the present-day. The absolute motion of the overriding plate is slow in comparison, migrating in the direction of the trench throughout its entire Cenozoic history. The absolute velocity of the overriding plate, is highest in the Eocene and decreases to an average of between 5 and 20 mm/yr thereafter until the present-day and approximates a stationary overriding plate.

4.6. Cascadia Subduction System

[62] The absolute motion of the downgoing and overriding plates along the Cascadia subduction zone is toward the trench with a reasonably high rate of motion for all times in the Cenozoic. The downgoing Farallon plate between 20 and 60 Ma has velocities of up to 110 mm/yr, but averages between 60 and 80 mm/yr (Figure 15). The inception of the Juan de Fuca plate at 20 Ma was associated with a sharp decrease in the absolute motion of downgoing plate in the north to about 20 mm/yr. The velocity of the downgoing plate increases again at 10 Ma to between 70 and 90 mm/yr.

[63] The overriding North American plate is moving in the direction of the trench throughout the Cenozoic at a smaller velocity than the downgoing Juan de Fuca and Farallon plates. The overriding plate reaches a maximum velocity of 45 mm/yr between 50 and 55 Ma and has a sharp decline after 40 Ma where the velocity sinks to 15 mm/yr (Figure 15). The absolute velocity of the overriding plate has remained stable at about 10–20 mm/yr over the past 25 m.y.

4.7. Middle America Subduction System

[64] The Middle America subduction system is characterized by fast velocities of the downgoing plate of up to 120 mm/yr between 35 and 60 Ma (Figure 16). In the north, the rate of motion of the downgoing plate steadily decreases to approximately 10 mm/yr in the past 10 m.y. However, in the central and southern Middle America trench, the downgoing plate is characterized by a sharp increase in the absolute plate velocity of between 90 and 150 mm/yr after 20 Ma. The present-day values are up to 100 mm/yr in the far south, adjacent to Costa Rica (Figure 16).

[65] The North American plate is the overriding plate at all times in the Cenozoic and its motion is always toward the trench, with minor changes in the magnitude of velocity over time. In the early Cenozoic, the overriding plate velocity was up to 80 mm/yr and greater than the downgoing plate velocity (Figure 16). After 50 Ma, the overriding plate velocity decreased to a relatively constant rate with an average of 20 mm/yr in the north and 10 mm/yr in the south.

4.8. Andes Subduction System

[66] The absolute motion of the downgoing and overriding plates along the Andes trench is characterized by the fast velocity of the downgoing plate toward the trench and the constant trenchward motion of the overriding South American plate (Figure 17). A similar pattern, but smaller in magnitude, is observed at the southern end of the Andes system. The downgoing plate velocity oscillates through time with peaks of 115 mm/yr between 40 and 55 Ma and another peak of 120 mm/yr between 15 and 25 Ma. The peaks in velocity of the downgoing plate coincide with the increase in the age of material being subducted along the trench and the break up of the Farallon

plate in the latter case. The absolute motion of the downgoing plate for the present-day ranges from 35 mm/yr in the north to 40–50 mm/yr in the central Andes to 10 mm/yr in the southern Andes (Figure 17).

[67] The overriding plate along the Andes is characterized by the fast trenchward motion of the South American plate with a maximum of 50 mm/yr in the early Cenozoic and later, a steady velocity of about 30 mm/yr in the north to 20 mm/yr in the central Andes. Along the southern Andes margin, the South American plate is moving toward the trench between 10 and 20 mm/yr throughout most of its history and in some instances is traveling toward the trench at a greater velocity than the downgoing plate (Figure 17). The fast motion of the overriding South American plate toward the trench causes extensive compression and subduction erosion along the Andean margin [*Lamb and Davis*, 2003]. The absolute motion of the overriding plate is forcing the rollback of the Andes subduction hinge.

4.9. Summary

[68] The absolute direction of motion of the overriding plate along the entire eastern Pacific margin is oriented toward the trench, with the fastest rates experienced adjacent to the South American plate along the Andes. A relatively fast motion of the overriding plate toward the trench results in a compressional strain regime on the overriding plate adjacent to the subduction boundary and extensive subduction erosion and compression is observed along the margin. In contrast, the absolute motion of the overriding plate along the western Pacific changes through time from being toward the trench (where we expect a compressional stress regime) to away from the trench resulting in an extensional stress regime. The change in direction of motion of the overriding plate, and hence the strain regime, is correlated with the onset of back-arc spreading on the overriding plate. This is best evidenced along the Tonga-Kermadec and Izu-Bonin-Mariana margins where the initiation of back-arc spreading in both the early Oligocene and late Miocene follows the same pattern. A first-order interpretation would suggest that the initiation of back-arc spreading on the overriding plate is controlled by the absolute motion of the overriding plate, as suggested by *Chase* [1978], *Scholz and Campos* [1995], and *Heuret and Lallemand* [2005]. However, the Java-Sunda trench is characterized by changes in the direction of motion of the overriding plate toward and away from the trench and back-arc spreading did not initiate along this margin during the motion of the plate away from the trench. In fact, along Sumatra and Java, there is evidence to suggest that significant folding and thrusting occurred during the Oligocene-Miocene [*Matthews and Bransden*, 1995; *Hall and Morley*, 2004], during the time when the overriding plate was moving away from the trench, even though we should expect an extensional stress regime on the overriding plate to facilitate the opening of the back-arc basins.

[69] The separation of subduction zones based on the strain regime on the overriding plate by *Jarrard* [1986] from highly compressional to highly extensional was found to be strongly related to the absolute motion of the overriding plate and the age of the subducting oceanic lithosphere. Our results concur with those of *Jarrard* [1986], as back-arc basins appear to initiate when the age of the subducting oceanic lithosphere is greater than 55 million years old and when the overriding plate is moving away from the trench.

5. Rollback of the Subduction Hinge

[70] Slab rollback is described as the seaward migration of the subduction hinge caused by the negative buoyancy and gravitational instability of the subducting slab as it founders and sinks into the underlying asthenosphere [*Molnar and Atwater*, 1978; *Dewey*, 1980; *Carlson and Melia*, 1984; *Garfunkel et al.*, 1986; *Faccenna et al.*, 2001]. Importantly, the sinking of the lithosphere due to its negative buoyancy occurs in both the parallel and perpendicular direction to the dip of the slab [*Molnar and Atwater*, 1978; *Schellart et al.*, 2003]. As a result, the slab naturally retreats away from the subduction hinge provided the overriding plate is moving seaward. *Carlson and Melia* [1984] and *Carlson and Mortera* [1990] found that if the overriding plate is migrating landward, hinge advancement will result. The rollback of the subduction hinge has been considered to be one of the primary mechanisms responsible for the development of back-arc extension. The negative buoyancy of the subducting slab due to the density of the material is believed to impart the greatest influence over the development and magnitude of slab rollback. Hence the age of the subducting oceanic lithosphere is believed to be a strong

control on rollback. However, previous studies [*Carlson et al.*, 1983; *Jarrard*, 1986; *Heuret and Lallemand*, 2005] found no clear correlation between the age of the subducting lithosphere and the rollback of the subduction hinge. *Jarrard* [1986] concluded that his data set was insufficient to conclusively rule out a rollback versus age correlation; however, the recent studies of *Heuret and Lallemand* [2005] and *Lallemand et al.* [2005] appear to support this conclusion. It is important to note that the data of *Jarrard* [1986] only included present-day values of rollback associated with back-arc basins.

[71] We have computed the amount of trench rollback along the Tonga-Kermadec, Izu-Bonin-Mariana and Japan-Kuril subduction systems by measuring the absolute motion of the overriding back-arc basin plate through time. Rollback rates were calculated at 500 km intervals along the strike of the trench for every 5 million years during the Cenozoic. The rates of back-arc spreading which are incorporated into the overriding plate velocities were taken from *Sdrolias et al.* [2003] for the SW Pacific, *Sdrolias et al.* [2004b] for the Philippine Sea plate, and the global age grids of *Müller et al.* [2005]. In the many regions where back-arc spreading is absent, the rollback of the subduction hinge is simply a measure of the absolute plate velocity of the overriding plate at a point along the subduction hinge line. The rollback of the subduction hinge through time is illustrated for each subduction zone in Figures 18a and 18b.

5.1. Tonga-Kermadec Subduction System

[72] The rollback of the subduction hinge along the Tonga-Kermadec trench (Figure 19) increases when spreading in the back-arc basin plate is active. Between 35 and 45 Ma, the rollback rate is a measure of the absolute motion of the Australian plate. However, after the initiation of back-arc spreading in the South Fiji Basin at ~33 Ma, the rollback rate is the motion of the Australian plate as well as the half-spreading rate of the South Fiji Basin. The rollback rate is initially slow (~45–50 mm/yr) compared to the motion of the overriding plate. The rollback rate increases after 30 Ma to be between 40 mm/yr in the south and 130 mm/yr to the north and is up to 110 mm/yr greater than the motion of the overriding plate. A similar increase in the rollback speed was observed with the initiation of spreading in the Lau Basin. The trench-normal rollback rate adjacent to the Lau Basin is up to 85 mm/yr, 70 mm/yr more than the motion of the overriding plate alone.

5.2. Izu-Bonin-Mariana Subduction System

[73] The rollback of the subduction hinge along the Izu-Bonin-Mariana trench (Figure 19) shows an increase during the Oligocene-early Miocene spreading in the Parece Vela and Shikoku Basins and the late Miocene opening of the Mariana Trough. The rollback rate at 30 Ma, just prior to the initiation of spreading in the Parece Vela and Shikoku Basins, is about 5 mm/yr away from the trench. When back-arc spreading develops, the rollback rate increases to 22 mm/yr. The spreading rate in the Parece Vela and Shikoku Basin increases after 25 Ma and this is expressed in a significant increase in the rollback rate to 95 mm/yr.

[74] After 20 Ma and the onset of clockwise rotation of the Philippine Sea plate, the rollback rate remains about 80 mm/yr but more closely resembles the magnitude of motion of the overriding plate. Spreading in the Mariana Trough is accompanied by a slight increase in the rollback speed [*Carlson and Mortera*, 1990].

5.3. Japan-Kuril Subduction System

[75] The rollback along the Japan-Kuril subduction system is a reflection of the absolute motion of the Eurasian plate between 35 and 60 Ma. Spreading in the Japan Sea was initiated at 30 Ma and corresponds to a slight increase in the rollback rates of the subduction hinge. The greatest rollback occurs between 15 and 25 Ma when the rate reaches 45 mm/yr, compared with the 15 mm/yr motion of the overriding Eurasian plate. In our calculations of rollback, we have not included the apparent opening of the Kuril Basin and Sea of Okhotsk to the north, as the age determination of these basins is uncertain and it is unclear whether or not they are floored with oceanic crust and/or extended continental crust. However, previous studies have suggested that these regions extended in the Oligocene-Eocene (Sea of Okhotsk) and spreading in the Kuril Basin in the mid/late Miocene [*Schellart et al.*, 2003]. If we assume that the initiation of extension occurred in the Eocene, adjacent to the northern Japan-Kuril trench, then we would expect to observe trench rollback occurring with an increase in magnitude in this region.

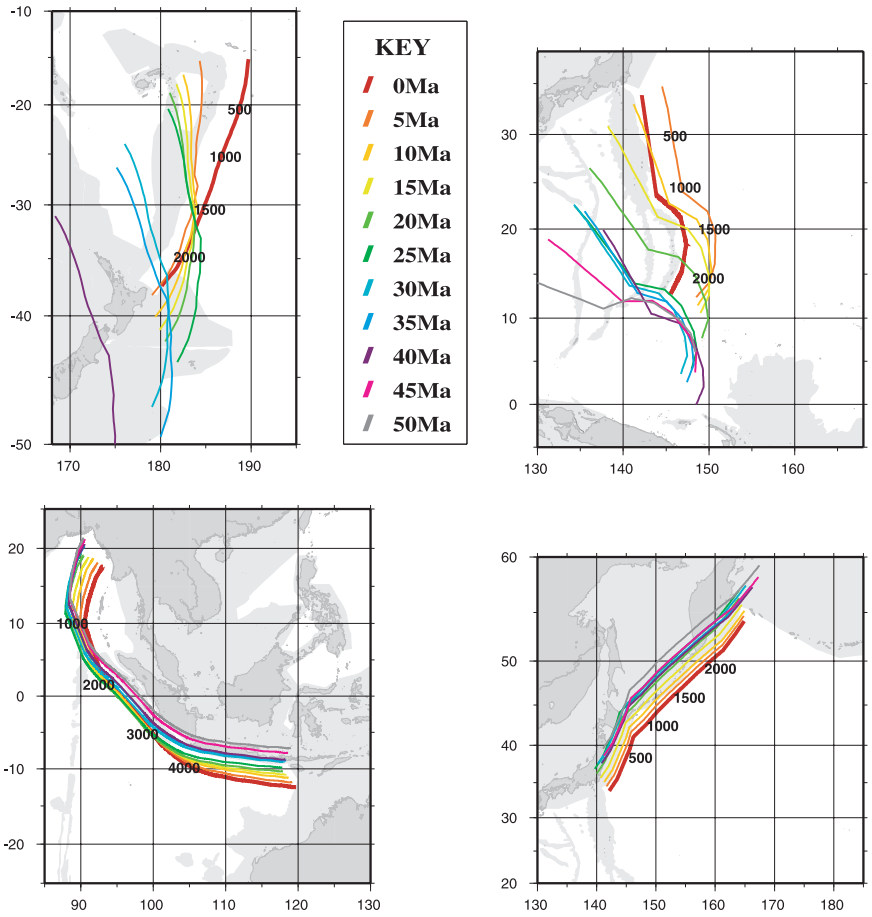

Figure 18a. Map view of the (top left) Tonga-Kermadec, (bottom left) Java-Sunda, (top right) Izu-Bonin-Mariana, and (bottom right) Japan-Kuril subduction systems with the reconstructed position of the trench plotted at 5 million year intervals. Thick red line denotes the present-day position of the trench and annotated numbers represent the points from where subduction parameters are taken (see Figures 2–9).

5.4. Summary

[76] Our results from the rollback of the subduction hinge and the absolute motion of the overriding plate (when back-arc spreading was not active) were compared to the age of the subducting lithosphere (Figure 19). The negative buoyancy of the subducting slab (which is a function of its age) is believed to be the primary influence on the magnitude of the rollback of the subduction hinge [*Molnar and Atwater*, 1978]. However, our results show no correlation between the age of the subducting lithosphere and rollback rate, implying no age dependence on the rollback of the subduction hinge. This result is not all that surprising as the rollback is a measure of the motion of the overriding and back-arc plates which are computed based on the spreading histories of the major ocean basins. The lack of age dependence on rollback rates was also noted by *Jarrard* [1986] and recently supported by *Lallemand et al.* [2005].

6. Dip Angle of the Subducting Slab

[77] The dip angle, shape and orientation of the subducting slab provides insights into subduction and back-arc basin dynamics but importantly, it is one of the crucial constraints for subduction-driven global mantle flow models. The properties of the subducting slab have been estimated from earthquake focal mechanisms and more recently from seismic tomography. The subducting slab, or seismic dipping zone, is believed to be primarily influenced by the density of the material entering the mantle (i.e., the age of the subducted oceanic lithosphere). Secondary factors, such as the motion

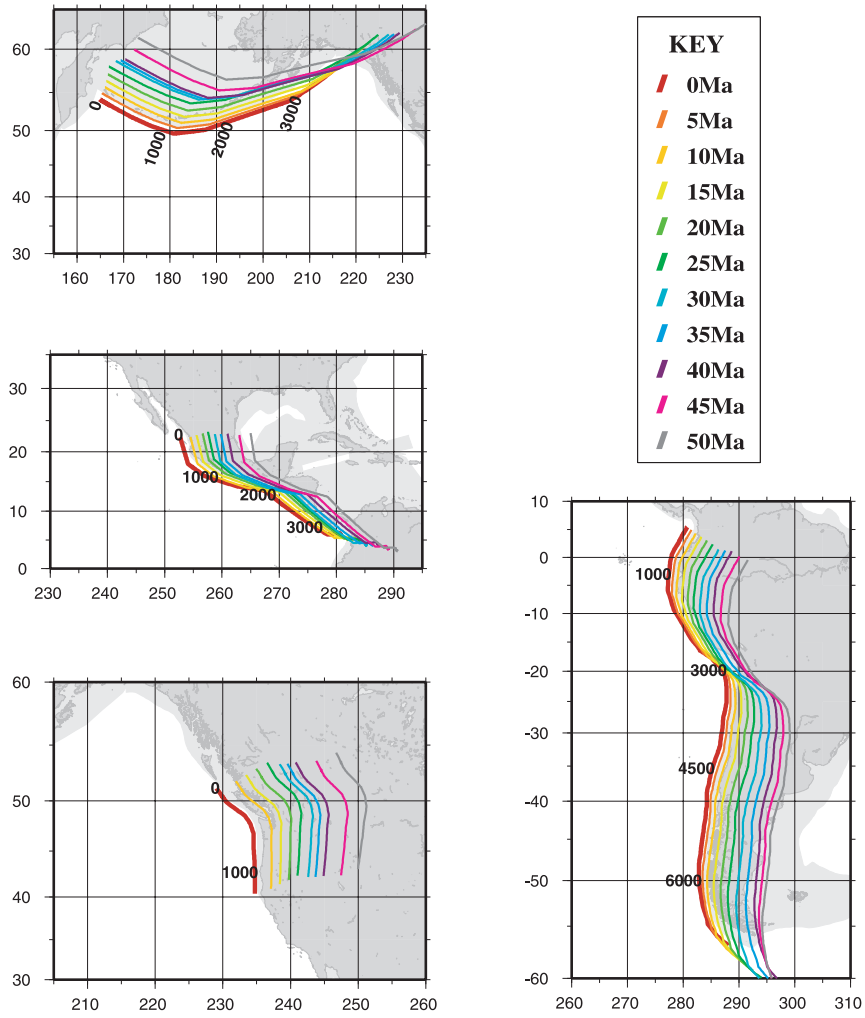

Figure 18b. Map view of the (top left) Aleutian, (middle left) Cascadia, (bottom left) Middle America, and (bottom right) Andes subduction systems with the reconstructed position of the trench plotted at 5 million year intervals. Thick red line denotes the present-day position of the trench, and annotated numbers represent the points from where subduction parameters are taken (see Figures 2–9).

of the overriding plate and the lateral mantle flow in the upper mantle may act to affect the natural sinking of the subducted material, thus affecting the angle at which this material sinks into the mantle. Previous studies [*Jarrard*, 1986; *Cruciani et al.*, 2005; *Lallemand et al.*, 2005] have attempted to establish a clear relationship between the dip of the slab and the age of the subducted oceanic lithosphere, whereby greater negative buoyancy of older oceanic lithosphere forces a steeper angle of sinking to develop. The study by *Cruciani et al.* [2005] suggests that no correlation exists between the age of subducting lithosphere and the dip of the slab (Figure 20).

[78] The dip angle of the subducting slab at each subduction zone was calculated using the slab depth contour data set of *Gudmundsson and Sambridge* [1998]. In previous studies of subduction parameters, a single dip measurement was obtained to represent the entire subduction margin (except in more recent papers by *Lallemand et al.* [2005] and *Cruciani et al.* [2005]). However, the dip of the slab can vary substantially along strike. We measured the dip angle of the subducting slab at every 100 km interval along the strike of each trench. At each 100 km point, we computed the distance between adjacent slab depth contours to calculate the intermediate dip angle (0–100 km depth) and the deep dip angle (150–400 km depth), following the convention of *Jarrard* [1986]. The dip angle calculations were taken normal to the strike of the trench, keeping this measurement consistent with the calculations of

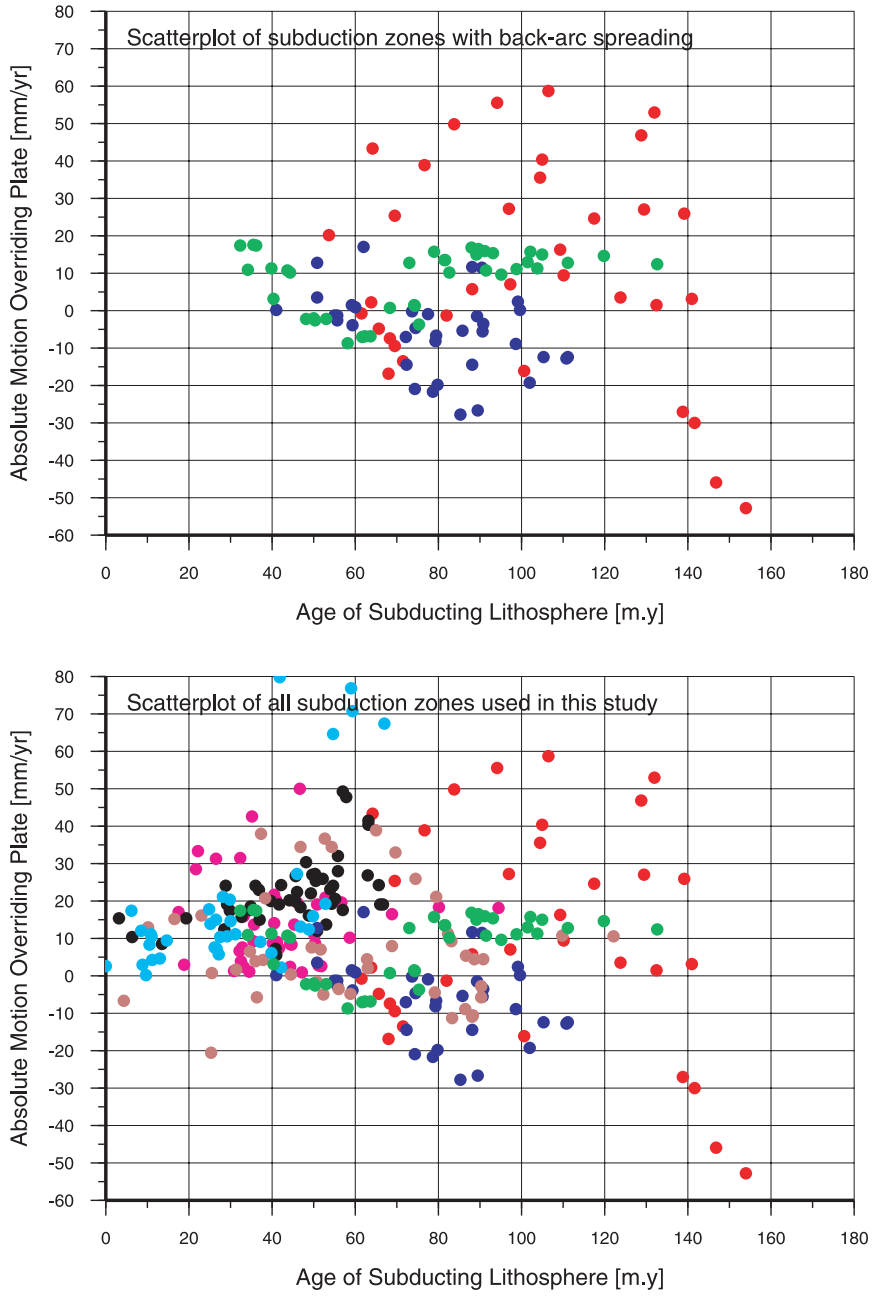

Figure 19. Scatterplot of the absolute motion of the overriding plate versus age of subducting lithosphere (top) for the three subduction systems identified as having an associated back-arc basin system and (bottom) for all the subduction zones used in this study. See Figure 20 for key to color code.

convergence rate and the absolute motion of the overriding and downgoing plates, which were taken normal to the trench. Dip measurements for the Cascadia subduction zone were not incorporated into our results due to the lack of a clearly defined seismic dipping zone at depth in this region.

[79] The intermediate dip angle (0–100 km depth) more accurately represents the age dependence (Figure 20) as the subducting slab acts as a rigid plate and maintains its shape at this depth and is not affected substantially by other factors. A regression analysis using a robust fit on the data was used to minimize the influence of outliers on the correlation coefficient. The data from the Izu-Bonin-Mariana and Middle America trench were excluded from this trend for reasons explained below. The deep dip (150–400 km depth) by comparison, should display no clear correlation

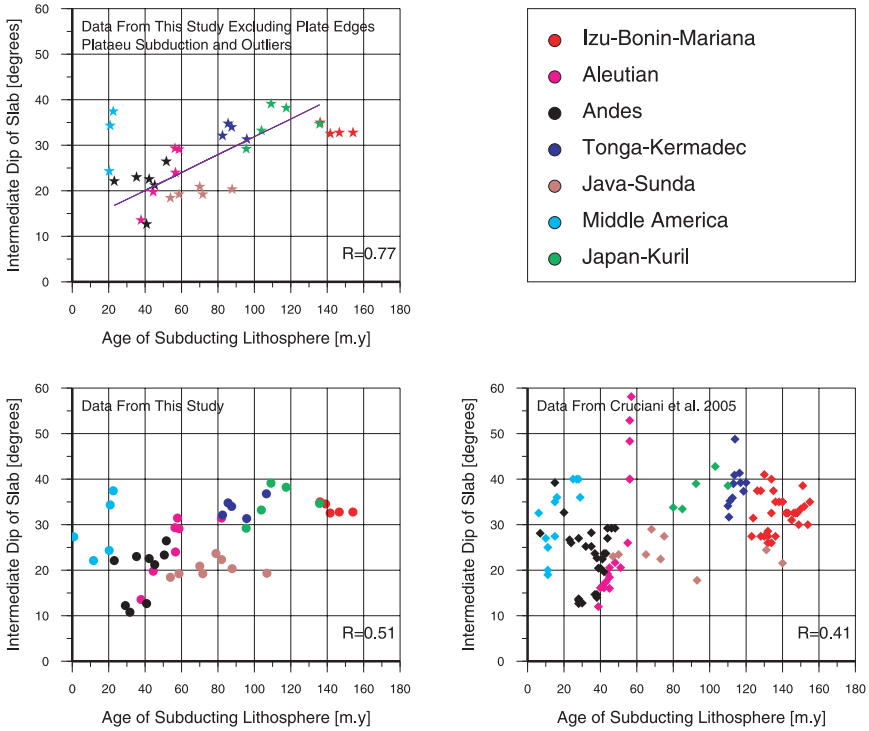

Figure 20. (bottom left) Intermediate slab dip versus age of the subducting lithosphere for the eight major subduction zones used in this study. The intermediate slab dip is taken as the first 100 km of the slab and is based on the method of *Jarrard* [1986]. (bottom right) Data from the study of *Cruciani et al.* [2005] plotted for comparison. (top left) Data from our study excluding the data from plate edges, plateau subduction, etc., from the method of *Lallemand et al.* [2005]. Thin purple line represents the best fit regression model with a robust fit. The correlation coefficient for each graph is displayed in the bottom right corner of each graph.

as lithosphere at this depth begins to lose its rigidity, shape and structure and is affected by changes in the mantle due to increases in the temperature and pressure at depth. The mean of the dip and the standard deviation was also calculated for each population.

[80] The analysis of results from the intermediate dip show that the intermediate dip of the slab (0–100 km) is dependent on the age of the subducting oceanic lithosphere (Figure 20). In the subduction systems where back-arc spreading is currently active (Izu-Bonin-Mariana and Tonga-Kermadec), the intermediate dip of the slab is between 30° and 40° (Figure 20) and agrees with the results of *Lallemand et al.* [2005]. The dip angle of the slab at these depths affects the size and location of the mantle wedge and presumably the rate at which the hinge will roll back. This age range also corresponds to the steepest dip angles of all subduction zones at this depth.

[81] The Middle America trench has a steeper slab than that predicted by its age. Although the crust being subducted at the Middle America trench is very young (0–20 Ma), the actual dip angle of the subducted slab is characteristic of 60–80 m.y. old crust. The convergence rate in this region is high and there is no obliquity in the convergence rate (Figure 8a). We believe that this very strong component of convergence normal to the trench forces the subducting slab into the mantle at a greater speed than for other subduction systems and hence produces a steeper slab for its age. Another anomalous system is the Izu-Bonin-Mariana where a shallower dip angle is observed compared to the age of the crust being subducted. The deep dip angle for the Izu-Bonin-Mariana trench is very steep, reaching 85°.

[82] The deep dip angle (150–400 km) versus age of the subducting oceanic lithosphere results in a scatterplot without correlation. However, we do observe a bimodal distribution of the deep dip values, with the two populations separated at about 65° (Figure 21). The shallower dip population includes the southern and central Japan-Kuril, northern and central Tonga-Kermadec and northern and central Andes trenches and has an average

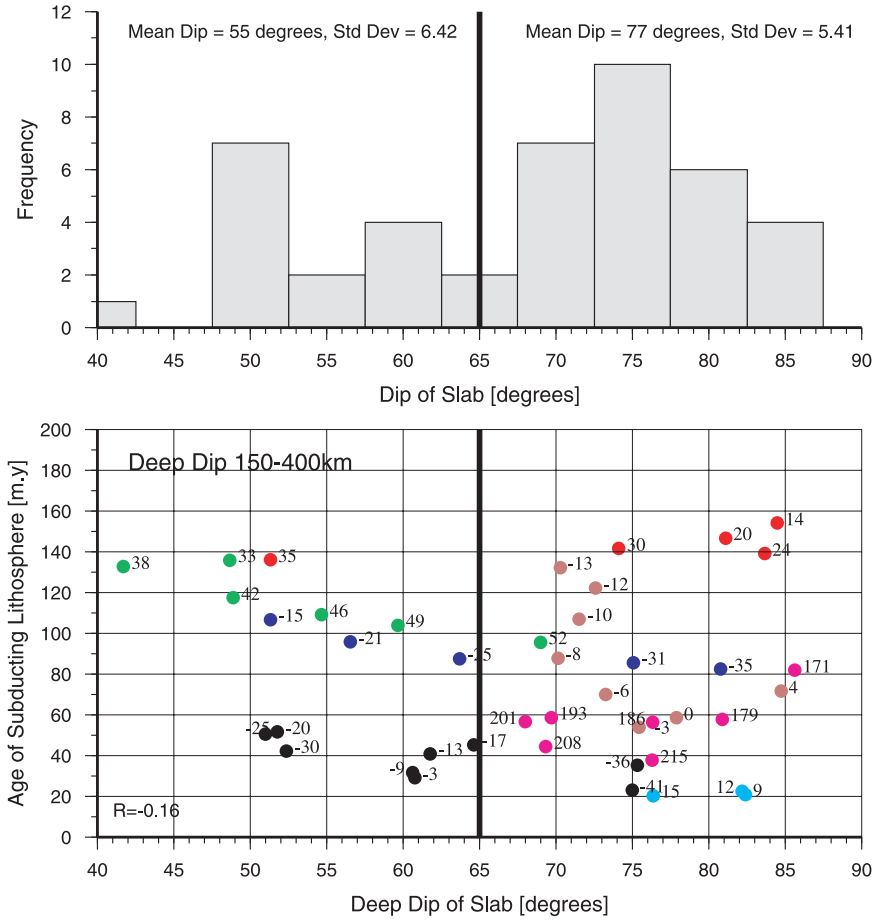

Figure 21. (bottom) Deep slab dip versus age of the subducting lithosphere for the eight major subduction zones used in this study. The deep slab dip is taken as the value between 150 and 400 km and is based on the method of *Jarrard* [1986]. The key is the same as in Figure 20. The numbers adjacent to the dots denote the latitudinal position of that point along the strike of the subduction zone (longitudinal position is taken for the Aleutian). (top) Normal distribution of the deep dip data. The two populations are clearly observed and separated at 65° by the thick black line. The mean dip and the standard deviation about the mean are displayed for each population.

deep dip value of 55°. The shallow dip along the Andes has been noted previously and is attributed to the young age of the oceanic crust being subducted along the trench as well as the subduction of aseismic ridges along its margin. The shallow dip along the northern Tonga-Kermadec trench can be explained by an upwelling beneath this region which has affected the subducted slab [*Gurnis et al.*, 2000] and can be observed in the S20RTS tomography model [*Ritsema et al.*, 1999] and mantle flow models [*Steinberger et al.*, 2004]. The shallow dip at the southern central Japan-Kuril trench may be influenced by the triple junction between the Izu-Bonin-Mariana, Japan-Kuril and Nankai trenches (see slab depth contours in Figure 5a) as well as sub-Pacific mantle pressure flow.

[83] The subduction zones found in the second population have a mean dip of 77° and are 22° steeper than the shallow population. We observe, even in the subduction zones with the steepest angles (Izu-Bonin-Mariana, Aleutians, Middle America), that the slab must be affected by other forces as the dips are shallower than 90° (Figure 21).

[84] Lateral mantle flow models in the lower upper mantle at about 500 km depth based on *Steinberger et al.* [2004] illustrate that the current direction of horizontal mantle flow along the rim of the Pacific is generally directed either landward or parallel to the subduction hinge. The flow of the mantle underneath the subducting slab would therefore result in a shallowing of the dip angle based on the forces applied to the subducting slab by the

regional mantle flow field. This may explain why the deep dip angles are shallower than expected in the vertical direction.

7. Discussion

[85] Subduction is a necessary prerequisite for back-arc extension to develop, however, back-arc extension is not associated with every subduction system. Many hypotheses exist to explain the mechanisms behind back-arc extension particularly the temporal and spatial distribution of back-arc extension. These proposed mechanisms include: the rollback of the subduction hinge [*Elsasser*, 1971; *Molnar and Atwater*, 1978; *Dewey*, 1980; *Faccenna et al.*, 2001; *Hall et al.*, 2003; *Schellart et al.*, 2003]; the absolute motion of the overriding plate [*Chase*, 1978; *Scholz and Campos*, 1995]; the effect of the sea anchor force [*Scholz and Campos*, 1995]; and various magmatic processes in the mantle wedge [*Karig*, 1971; *Sleep and Toksoz*, 1971].

[86] The major outcomes of our time- and space-dependent study on our selected subduction zones include the following.

[87] 1. The initiation of back-arc spreading, both in the present day and in the past, only occurs when the age of the subducting oceanic lithosphere is greater than 55 million years in those subduction zones that subduct normal oceanic crust and fit the criteria outlined earlier.

[88] 2. The initiation of back-arc extension is preceded by the landward migration of the overriding plate, in an absolute reference frame.

[89] 3. After the initiation of back-arc extension, the development of the back-arc spreading system persists regardless of whether the overriding plate continues to move away from the trench or if it changes direction and migrates toward the trench.

[90] 4. The cessation of spreading in the back-arc region is not dependent on the age of the subducting lithosphere or the motion of the overriding plate.

[91] 5. There is no correlation between the age of the subducting lithosphere and the rollback speed of the subduction hinge (Figure 19). However, as expected, the rollback speed increases substantially once back-arc spreading is established.

[92] 6. The dip angle of the subducting slab can be correlated with the age of subducting lithosphere for depths between 0 and 100 km (Figure 20). Back-arc extension occurs at subduction systems with an intermediate dip angle steeper than 30°. No correlation is observed between the deep dip angle and the age of the subducting lithosphere (Figure 21) as the slab at this depth is affected by the landward lateral flow of the upper mantle exerting a lateral force on the subducting slab.

[93] The abovementioned outcomes do not hold true for several subduction zones which we excluded from our study. The subduction zones of SE Asia and north of Australia and the New Hebrides subduction system subduct anomalous oceanic, hybrid or continental crust. The crust subducting at the Sandwich subduction zone is normal oceanic crust and younger than 55 m.y. However, this young crust formed at a superslow spreading ridge (South American–Antarctic Ridge) and it is well established that super slow spreading crust is anomalously cold at a given age compared to oceanic crust created at normal spreading rates [*Henstock et al.*, 1993; *Phipps Morgan and Chen*, 1993]. Therefore we believe that the exclusion of these subduction zones from our study and results is warranted.

[94] It must be noted that the vast amount of data presented in this study is associated with various errors, which cannot easily be quantified. In particular, the age of the subducting lithosphere and velocity of the plates in both and relative and absolute sense, are associated with errors in the plate reconstructions of the region, in the interpretation of the magnetic anomalies and in the errors inherent in the timescale used.

[95] Our results suggest that the initiation of back-arc extension in subduction zones that subduct normal oceanic lithosphere, occurs when the age of the subducting oceanic lithosphere is greater than 55 million years. This condition is satisfied for all subduction zones investigated here during the entire Cenozoic. The formation of the South Fiji Basin at 33 Ma along the Tonga-Kermadec trench was associated with the subduction of 52–90 m.y. old Pacific lithosphere (Figures 2b and 10), the formation of the Parece Vela and Shikoku Basins at 30 Ma along the Izu-Bonin-Mariana trench was associated with the subduction of 65–100 m.y. old Pacific lithosphere (Figures 4b and 12) and the formation of the Japan Sea along the Japan-Kuril trench was associated with the subduction of 70 m.y. old Pacific lithosphere (Figures 5b and 13). The present-day formation of the Lau Basin and Mariana Trough is associated with subducting

oceanic lithosphere greater than 90 m.y. Conversely, the entire eastern Pacific margin (Cascadia, Middle America, Andes) has an absence of back-arc extension on the overriding plate and the subducting oceanic lithosphere is generally under 50 million years. The age as well as the dip of the slab alone do not control the formation of back-arc extension as some subduction zones (e.g., Java-Sunda, Aleutian) have subducted oceanic lithosphere older than 55 million years at some time in the past with no resultant back-arc extension.

[96] We also examined the relationship between the age of the subducting lithosphere and the rollback of the subduction hinge (Figure 19) to assess the hypothesis that the rollback of the subduction hinge is the major driving force for back-arc extension. Back-arc extension was recently modeled using analogue experiments [*Faccenna et al.*, 2001; *Schellart et al.*, 2002; *Schellart et al.*, 2003] as a dynamic consequence of rapid hinge rollback. The numerical model of *Hall et al.* [2003] showed that rapid rollback of the subduction hinge is caused by the increase in the buoyancy force and the steepening of the subducting slab [*Hall et al.*, 2003]. Our results, however, found no correlation between the age of the subducting oceanic lithosphere and the speed of hinge rollback, concurring with the study of present-day kinematics by *Jarrard* [1986] and *Lallemand et al.* [2005]. This suggests the rollback of the subduction hinge is not directly controlled by the age of the subducting slab. However, once back-arc spreading has been established, the rollback of the subduction hinge is largely determined by the spreading history of the seaward back-arc basin plate and the dip of the slab. The continuation of hinge rollback and accompanied back-arc extension, as predicted by the dynamic models of *Hall et al.* [2003], is driven by the vertical descent of the slab due to the dominance of the slab buoyancy force.

[97] The hypothesis that the driving mechanism of back-arc extension is purely related to the absolute motion of the overriding plate causing accommodation space to form on the overriding plate when the plate is moving landward was previously proposed by *Chase* [1978] and *Scholz and Campos* [1995]. Additionally, *Scholz and Campos* [1995] hypothesized that the sea anchor force is the dominant force responsible for the formation of back-arc spreading. The sea anchor force is a force exerted laterally on the subducting slab which acts to resist its motion, hence "anchoring" the slab in the mantle. Back-arc spreading is believed to result if the upper plate velocity is moving in the opposite direction to the subducting slab (i.e., landward). In this situation the force will drag down the slab, causing the resultant extension on the overriding plate. Compression and deformation on the overriding plate will result if the sea anchor force acts to push the slab upward. The study by *Scholz and Campos* [1995] implies that the overriding plate must be moving away from the trench both at the initiation of back-arc spreading as well as during the entire spreading history as the state of stress on the overriding plate is controlled by the sea anchor force.

[98] Our results show that when subducting oceanic lithosphere is older than 55 million years, back-arc extension is preceded by the landward migration of the overriding plate or in some cases, the stationary position of the overriding plate. However, during back-arc spreading, the overriding plate may move away from the trench or toward the trench. Prior to the initiation of spreading in the South Fiji Basin, the overriding Australian plate began to move away from the trench and this continued throughout the development of the South Fiji Basin. The overriding plate was still moving away from the trench even at the cessation of spreading at 25 Ma. Along the Izu-Bonin-Mariana trench, the overriding Philippine Sea plate was moving away from the trench prior to the initiation of spreading in the Parece Vela and Shikoku Basins at 30 Ma. However, during back-arc spreading, the overriding plate underwent trenchward motion (at 25 Ma) and continued to migrate toward the trench until the cessation of spreading at 15 Ma. The initiation of spreading in the Japan Sea at 30 Ma also corresponds to the landward migration of the overriding plate. However, 5 million years after the initiation of this basin, the overriding plate was again moving toward the trench and even after the cessation of back-arc spreading at ~15 Ma.

[99] The motion of the overriding plate away from the trench prior to the initiation of back-arc spreading agrees with the model of *Chase* [1978] and *Scholz and Campos* [1995]. However, this only holds true for the initial stages of back-arc basin development. Along the eastern Pacific margin, the overriding plate is moving toward the trench at all times in the Cenozoic and no resultant back-arc extension forms. In fact, this margin is dominated by compression, deformation and subduction erosion.

[100] The cessation of back-arc spreading and the apparent episodicty of back-arc spreading does not appear to be controlled by the upper plate velocities, nor the age of the subducting oceanic lithosphere. *Faccenna et al.* [2001] suggest that the episodicity results from the inability of the subducting slab to penetrate the 670 km discontinuity, thus slowing down the convergence rate and trench migration. Alternatively, *Schellart* [2005] suggests that episodic back-arc extension is caused by changes from periods of hinge retreat and hinge advancement causing the slab to fold over at the transition zone. However, our results do not show a decrease in the convergence rate at any of our back-arc basin regions (Figures 10, 12, and 13). We observe a decrease in the hinge migration (Figures 19, 21, and 22) as a consequence of the cessation of back-arc spreading. The reasons for the cessation of back-arc spreading and the episodicity of back-arc spreading requires further analysis of mantle dynamics in a region where several episodes of back-arc spreading are associated with a retreating subduction hinge.

8. Conclusions

[101] We have compiled and examined a detailed set of subduction and back-arc basin parameters based on a new plate motion model and the global paleo-age grid data set. We have found that the driving mechanism for back-arc extension involves a combination of surface kinematics, properties of the downgoing slab and the effect of the lateral mantle flow on the subducting slab. An evaluation of previously proposed models has failed to equivocally demonstrate that any model is representative of back-arc basin dynamics.

[102] The age of the subducting lithosphere is an important primary constraint on back-arc spreading. The negative buoyancy of the downgoing slab affects the dip angle of the subducting slab in the upper mantle as well as the interaction between the slab and the lateral flow of the mantle. Back-arc spreading only occurs when the age of the subducting lithosphere is greater than 55 million years at subduction zones associated with normal oceanic lithosphere. This appears to be an essential condition which must be satisfied for back-arc extension to develop. Associated with the age of the lithosphere is the intermediate dip angle of the slab. Once the subducting slab has reached a critical intermediate dip angle of 30° and the age of the subducting lithosphere is greater than 55 m.y., back-arc spreading will be able to initiate if the overriding plate is moving away from the trench. The motion of the overriding plate away from the trench leads to the creation of accommodation space on the overriding plate. The mechanism creating the accommodation space maybe a combination of the passive rollback of the subduction hinge and the mantle flow dragging the subducting slab downward and causing extension on the overriding plate. The locus of back-arc extension occurs along the rheologically weakest part of the trench-arc–back-arc system. This is commonly in between the remnant and active volcanic arc. However, if another part of the system is sufficiently heated by a mantle plume, for example Norfolk Basin [*Sdrolias et al.*, 2004a], then the locus of back-arc extension may be transferred to a region of weakened crust. The creation of accommodation space on the overriding plate is purely driven by upper plate kinematics.

[103] After the initiation of back-arc spreading, we observe an increase in the rollback rate of the subduction hinge with the amount of accommodation space created on the overriding plate determined by the spreading history of the back-arc basin plate. The rollback of the subduction hinge becomes the dominant mechanism driving back-arc spreading once it is initiated. Back-arc basin formation will continue unabated even if the overriding plate begins to move toward the trench as the rollback of the subduction hinge ensures that there is sufficient accommodation space for the persistence of back-arc spreading. However, if the overriding plate continues to migrate away from the trench, relatively faster spreading rates are observed in the back-arc basin, as expected. The cessation of back-arc spreading cannot be correlated with any surface kinematic events. We suggest that the interaction of the subducting slab and changes in lateral mantle flow may be responsible for the cessation in back-arc spreading. However, it would be necessary to examine paleomantle flow field models at the time of back-arc spreading cessation to understand the effect that the lateral mantle flow plays on the dip of the subducting slab. We hypothesize that an increase in the speed of landward flow of the mantle underneath the subducting slab may be a potential trigger for the cessation in back-arc spreading.

[104] The suggestion that back-arc basin formation is purely controlled by the motion of the overriding plate [*Chase*, 1978; *Scholz and Campos*, 1995] does not concur with our results of subduction and back-arc basin kinematics. Although the motion of

the overriding plate at the time of back-arc initiation correlates with the formation of back-arc extension, it does not succeed in predicting the further development of the back-arc system. Similarly, the notion that the rollback of the subduction hinge driven by the age of the subducting lithosphere is the driving mechanism for back-arc extension does not adequately explain why some regions with sufficiently old crust do not form an associated back-arc basin or why there is no correlation between the age of the subducting lithosphere and the speed of rollback.

[105] The data that we have presented in this study can be incorporated into both simple 2D and complex 3D numerical models of subduction zones and whole Earth mantle motion models as surface constraints on the structure of the subducting slab and the velocities of the tectonic plates. The mantle must play an important part in back-arc basin dynamics and the exploration of its role in affecting the dip of the slab will help resolve the outstanding issues. Our subduction zone and back-arc basin parameters will prove invaluable to any scientist interested in the dynamics of the subduction factory. The data can be used in conjunction with field geological data to explore the genesis and development of volcanic arc chains, the fluxes of seawater volatiles subducted at the trench, or mantle convection models, for example. It can also be used to predict or understand the location of volcanic rocks associated with different types of convergent plate margins.

[106] Further data and results can be viewed at http://www.earthbyte.org.

Acknowledgments

[107] We would like to thank Wouter Schellart and Serge Lallemand for very thorough and useful reviews of the manuscript which helped improve its quality and clarity. Mike Gurnis, Walter Roest, and Nick Mortimer are thanked for reviews of early drafts of the manuscript. Thank you also goes to Bernhard Steinberger for access to his global mantle flow models and Carmen Gaina for her contributions to the paleoage grids. All figures, graphs, and statistical analysis in this study were created using the GMT software package [*Wessel and Smith*, 1998].

References

Baker, M. B., T. L. Grove, and R. Price (1994), Primitive basalts and andesites from the Mt. Shasta region, N. California: Products of varying melt fraction and water content, *Contrib. Mineral. Petrol.*, *118*, 111–129.

Ben-Avraham, Z., and S. Uyeda (1983), Entrapment origin of marginal seas, in *Geodynamics of the Western Pacific-Indonesian Region*, *Geodyn. Ser.*, vol. 11, edited by T. W. C. Hilde and S. Uyeda, pp. 91–104, AGU, Washington, D. C.

Bevis, M., et al. (1995), Geodetic observations of very rapid convergence and back-arc extension at the Tonga Arc, *Nature*, *374*, 249–251.

Billen, M. I., and J. M. Stock (2000), Morphology and origin of the Osbourn Trough, *J. Geophys. Res.*, *105*, 13,481–13,489.

Bird, P. (2003), An updated digital model of plate boundaries, *Geochem. Geophys. Geosyst.*, *4*(3), 1027, doi:10.1029/2001GC000252.

Bloomer, S., et al. (1995), Early Arc volcanism and the ophiolite problem: A perspective from drilling in the western Pacific, in *Active Margins and Marginal Basins of the Western Pacific*, *Geophys. Monogr. Ser.*, vol. 88, edited by B. Taylor and J. Natland, pp. 1–30, AGU, Washington, D. C.

Borg, L. E., M. A. Clynne, and T. D. Bullen (1997), The variable role of slab-derived fluids in the generation of a suite of primitive calc-alkaline lavas from the southernmost Cascades, California, *Can. Mineral.*, *35*, 425–452.

Cande, S. C., J. M. Stock, R. D. Müller, and T. Ishihara (2000), Cenozoic motion between East and West Antarctica, *Nature*, *404*, 145–150.

Carlson, R. L., and C. N. Herrick (1990), Densities and porosities in the oceanic crust and their variations with depth and age, *J. Geophys. Res.*, *95*, 9153–9170.

Carlson, R. L., and P. J. Melia (1984), Subduction hinge migration, *Tectonophysics*, *102*, 399–411.

Carlson, R. L., and G. C. A. Mortera (1990), Subduction hinge migration along the Izu-Bonin-Mariana Arc, *Tectonophysics*, *181*, 331–344.

Carlson, R. L., T. W. C. Hilde, and S. Uyeda (1983), The driving mechanism of plate tectonics: Relation to age of lithosphere at trenches, *Geophys. Res. Lett.*, *10*, 297–300.

Chamot-Rooke, N., C. Rangin, and C. Neilsen (2001), Timing and kinematics of Andaman Basin opening, *Eos Trans. AGU*, *82*(20), Spring Meet. Suppl., Abstract T42B-08.

Chase, C. G. (1978), Extension behind island arcs and motions relative to hotspots, *J. Geophys. Res.*, *83*, 5380–5387.

Cruciani, C., E. Carminati, and C. Doglioni (2005), Slab dip vs. lithospheric age: No direct function, *Earth Planet. Sci. Lett.*, *238*, 298–310.

Deschamps, A., and S. Lallemand (2002), The West Philippine Basin: An Eocene to early Oligocene back arc basin opened between two opposed subduction zones, *J. Geophys. Res.*, *107*(B12), 2322, doi:10.1029/2001JB001706.

Dewey, J. F. (1980), Episodicity, sequence and style at convergent plate boundaries, in *The Continental Crust and Its Mineral Deposits*, edited by D. W. Strange, *Geol. Assoc. Can. Spec. Pap.*, *20*, 553–573.

Elsasser, W. M. (1971), Seafloor spreading as thermal convection, *J. Geophys. Res.*, *76*, 1101–1112.

Engebretson, D. C., A. Cox, and R. G. Gordon (1986), Relative motions between oceanic and continental plates in the Pacific basin, *Spec. Pap. Geol. Soc. Am.*, *206*, 1–59.

Faccenna, C., F. Funiciello, D. Giardini, and P. Lucente (2001), Episodic back-arc extension during restricted mantle convection in the central Mediterranean, *Earth Planet. Sci. Lett.*, *187*, 105–116.

Gaina, C., and R. D. Müller (2004), Global oceanic crust production since mid-Cretaceous based on paleo-seafloor age grids, paper presented at the GSA Annual Meeting, Geol. Soc. of Am., Denver, Colo.

Garfunkel, Z., C. D. Anderson, and G. Schubert (1986), Mantle circulation and the lateral migration of subducted slabs, *J. Geophys. Res.*, *91*, 7205–7223.

Grellet, C., and J. Dubois (1982), The depth of trenches as a function of the subduction rate and age of the lithosphere, *Tectonophysics*, *82*, 45–56.

Gudmundsson, O., and M. Sambridge (1998), A regionalized upper mantle (RUM) seismic model, *J. Geophys. Res.*, *103*, 7121–7136.

Gurnis, M., J. Ritsema, and H. J. van Heijst (2000), Tonga Slab deformation: The influence of a lower mantle upwelling on a slab in a young subduction zone, *Geophys. Res. Lett.*, *27*, 2373–2376.

Gurnis, M., C. E. Hall, and L. L. Lavier (2004), Evolving force balance during incipient subduction, *Geochem. Geophys. Geosyst.*, *5*, Q07001, doi:10.1029/2003GC000681.

Hall, C. E., M. Gurnis, M. Sdrolias, L. L. Lavier, and R. D. Müller (2003), Catastrophic initiation of subduction following forced convergence across fracture zones, *Earth Planet. Sci. Lett.*, *212*, 15–30.

Hall, R., and C. K. Morley (2004), Sundaland basins, in *Continent-Ocean Interactions Within East Asian Marginal Seas*, *Geophys. Monogr. Ser.*, vol. 149, edited by P. Clift et al., pp. 55–85, AGU, Washington, D. C.

Hall, R., J. R. Ali, C. D. Anderson, and S. J. Baker (1995), Origin and motion history of the Philippine Sea Plate, *Tectonophysics*, *251*, 229–250.

Heestand, R. L., and S. T. Crough (1981), The effect of hotspots on the oceanic age-depth relation, *J. Geophys. Res.*, *86*, 6107–6114.

Heine, C., R. D. Müller, and C. Gaina (2004), Reconstructing the lost eastern Tethys Ocean Basin: Convergence history of the SE Asian margin and marine gateways, in *Continent-Ocean Interactions Within East Asian Marginal Seas*, *Geophys. Monogr. Ser.*, vol. 149, edited by P. Clift et al., pp. 37–54, AGU, Washington, D. C.

Henstock, T. J., A. W. Woods, and R. S. White (1993), The accretion of oceanic crust by episodic sill intrusion, *J. Geophys. Res.*, *98*, 4143–4162.

Heuret, A., and S. Lallemand (2005), Plate motions, slab dynamics and back-arc deformation, *Phys. Earth Planet. Inter.*, *149*, 31–51.

Hilde, T. W. C., and C. S. Lee (1984), Origin and evolution of the West Philippine Basin: A new interpretation, *Tectonophysics*, *102*, 85–104.

Jarrard, R. D. (1986), Relations among subduction parameters, *Rev. Geophys.*, *24*, 217–284.

Johnston, S. T., and D. J. Thorkelson (1997), Cocos-Nazca slab window beneath Central America, *Earth Planet. Sci. Lett.*, *146*, 465–474.

Jolivet, L., K. Tamaki, and M. Fournier (1994), Japan Sea, opening history and mechanism: A synthesis, *J. Geophys. Res.*, *99*, 22,237–22,259.

Jurdy, D. M. (1979), Relative plate motions and the formation of marginal basins, *J. Geophys. Res.*, *84*, 6796–6802.

Karig, D. E. (1971), Origin and development of marginal basins in the western Pacific, *J. Geophys. Res.*, *76*, 2542–2561.

Kelemen, P. B., G. M. Yogodzinski, and D. W. Scholl (2003), Along-strike variation in the Aleutian Island Arc: Genesis of high Mg# andesite and implications for continental crust, in *Inside the Subduction Factory*, *Geophys. Monogr. Ser.*, vol. 138, edited by J. Eiler, pp. 223–276, AGU, Washington, D. C.

Kirby, S. H., W. B. Durham, and L. A. Stern (1991), Mantle phase changes and deep earthquake faulting in subducting lithosphere, *Science*, *252*, 216–225.

Lagabrielle, Y., J. Goslin, H. Martin, J.-L. Thirot, and J. M. Auzende (1997), Multiple active spreading centres in the hot North Fiji Basin (southwest Pacific): A possible model for Archaean seafloor dynamics?, *Earth Planet. Sci. Lett.*, *149*, 1–13.

Lallemand, S., A. Heuret, and D. Boutelier (2005), On the relationships between slab dip, back-arc stress, upper plate absolute motion, and crustal nature in subduction zones, *Geochem. Geophys. Geosyst.*, *6*, Q09006, doi:10.1029/2005GC000917.

Lamb, S., and P. Davis (2003), Cenozoic climate change as a possible cause for the rise of the Andes, *Nature*, *425*, 792–797.

Lee, T. Y., and L. A. Lawver (1995), Cenozoic plate reconstructions of southeast Asia, *Tectonophysics*, *251*, 85–138.

Liu, C. S., J. R. Curray, and J. M. McDonald (1983), New constraints on the tectonic evolution of the eastern Indian Ocean, *Earth Planet. Sci. Lett.*, *65*, 331–342.

Lonsdale, P. (1988), Paleogene history of the Kula Plate: Offshore evidence and onshore implications, *Geol. Soc. Am. Bull.*, *100*, 733–754.

Martinez, F., and B. Taylor (2002), Mantle wedge control on back-arc crustal accretion, *Nature*, *416*, 417–420.

Martinez, F., P. Fryer, N. A. Baker, and T. Yamazaki (1995), Evolution of backarc rifting: Mariana Trough, 20°–24°N, *J. Geophys. Res.*, *100*, 3807–3827.

Matthews, S. J., and P. J. E. Bransden (1995), Late Cretaceous and Cenozoic tectono-stratigraphic development of the East Java Sea Basin, *Mar. Pet. Geol.*, *12*, 499–510.

Molnar, P., and T. Atwater (1978), Interarc spreading and Cordilleran tectonics as alternatives related to the age of subducted oceanic lithosphere, *Earth Planet. Sci. Lett.*, *41*, 330–340.

Molnar, P., D. Freedman, and J. S. F. Shih (1979), Lengths of Intermediate and deep seismic zones and temperatures in downgoing slabs of lithosphere, *Geophys. J. R. Astron. Soc.*, *56*, 41–54.

Müller, R. D., J.-Y. Royer, and L. A. Lawver (1993), Revised plate motions relative to the hotspots from combined Atlantic and Indian Ocean hotspot tracks, *Geology*, *16*, 275–278.

Müller, R. D., C. Gaina, M. Sdrolias, and C. Heine (2005), Reconstructing vanished ocean basins, paper presented at the European Geophysical Union Annual Meeting, Vienna.

Nakanishi, M., K. Tamaki, and K. Kobayashi (1989), Mesozoic magnetic anomaly lineations and seafloor spreading history of the northwestern Pacific, *J. Geophys. Res.*, *94*, 15,437–15,462.

Okino, K., S. Kasuga, and Y. Ohara (1998), A new scenario of the Parece Vela Basin genesis, *Mar. Geophys. Res.*, *20*(1), 21–40.

O'Neill, C. J., R. D. Müller, and B. Steinberger (2005), On the uncertainties in hotspot reconstructions and the significance of moving hotspot reference frames, *Geochem. Geophys. Geosyst.*, *6*, Q04003, doi:10.1029/2004GC000784.

Parsons, B., and J. C. Sclater (1977), An analysis of the variation of ocean floor bathymetry and heat flow with age, *J. Geophys. Res.*, *82*, 803–827.

Phipps Morgan, J., and Y. J. Chen (1993), Dependence of ridge-axis morphology on magma supply and spreading rate, *Nature*, *364*, 706–708.

Replumaz, A., and P. Tapponnier (2003), Reconstruction of the deformed collision zone between India and Asia by backward motion of lithospheric blocks, *J. Geophys. Res.*, *108*(B6), 2285, doi:10.1029/2001JB000661.

Ritsema, J., H. J. van Heijst, and J. H. Woodhouse (1999), Complex shear wave velocity structure imaged beneath Africa and Iceland, *Science*, *286*, 1925–1928.

Ruff, L. J., and H. Kanamori (1980), Seismicity and the subduction process, *Phys. Earth Planet. Inter.*, *23*, 240–252.

Schellart, W. P. (2005), Influence of the subducting plate velocity on the geometry of the slab and migration of the subduction hinge, *Earth Planet. Sci. Lett.*, *231*, 197–219.

Schellart, W. P., G. S. Lister, and M. N. Jessell (2002), Analogue modeling of arc and backarc deformation in the New Hebrides Arc and north Fiji Basin, *Geology*, *30*, 311–314.

Schellart, W. P., M. N. Jessell, and G. S. Lister (2003), Asymmetric deformation in the backarc region of the Kuril Arc, northwest Pacific: New insights from analogue modeling, *Tectonics*, *22*(5), 1047 doi:10.1029/2002TC001473.

Scholz, C. H., and J. Campos (1995), On the mechanism of seismic decoupling and back-arc spreading at subduction zones, *J. Geophys. Res.*, *100*, 22,103–22,115.

Sclater, J. G. (1972), Heat flow and elevation of the marginal basins of the western Pacific, *J. Geophys. Res.*, *77*, 5705–5719.

Sdrolias, M., R. D. Müller, and C. Gaina (2003), Tectonic evolution of the SW Pacific using constraints from back-arc basins, in *The Evolution and Dynamics of the Australian Plate*, edited by R. Hillis and R. D. Müller, *Spec. Pap. Geol. Soc. Am.*, *372*, 343–359.

Sdrolias, M., R. D. Müller, A. Mauffret, and G. Bernardel (2004a), Enigmatic formation of the Norfolk Basin, SW Pacific: A plume influence on back-arc extension, *Geochem. Geophys. Geosyst.*, *5*, Q06005, doi:10.1029/2003GC000643.

Sdrolias, M., W. R. Roest, and R. D. Müller (2004b), An expression of Philippine Sea plate rotation: The Parece Vela and Shikoku basins, *Tectonophysics*, *394*, 69–86.

Severinghaus, J., and T. Atwater (1990), Cenozoic geometry and thermal state of the subducting slabs beneath western North America, in *Basin and Range Extensional Tectonics Near the Latitude of Las Vegas Nevada*, edited by B. P. Wernicke, *Mem. Geol. Soc. Am.*, *176*, 1–22.

Sleep, N. H., and M. N. Toksoz (1971), Evolution of marginal seas, *Nature*, *233*, 548–550.

Stein, C. A., and S. Stein (1992), A model for the global variation in oceanic depth and heat flow with lithospheric age, *Nature*, *359*, 123–129.

Stein, S., and C. A. Stein (1996), Thermo-mechanical evolution of oceanic lithosphere: Implications for the subduction process and deep earthquakes, in *Subduction Top to Bottom*, *Geophys. Monogr. Ser.*, vol. 96, edited by G. E. Bebout et al., pp. 1–18, AGU, Washington, D. C.

Steinberger, B., R. Sutherland, and R. J. O'Connell (2004), Prediction of Emperor-Hawaii seamount locations from a revised model of global plate motion and mantle flow, *Nature*, *430*, 167–173.

Stern, R. A., and S. H. Bloomer (1992), Subduction zone infancy: Examples from the Eocene Izu-Bonin-Mariana and Jurassic California arcs, *Geol. Soc. Am. Bull.*, *104*, 1621–1636.

Stern, R. J. (2002), Subduction zones, *Rev. Geophys.*, *40*(4), 1012, doi:10.1029/2001RG000108.

Taylor, B., K. Zellmer, F. Martinez, and A. Goodlife (1996), Sea-floor spreading in the Lau Back-arc Basin, *Earth Planet. Sci. Lett.*, *144*, 35–40.

Uyeda, S. (1977), Some basic problems in the trench-arc-back-arc system, in *Island Arcs, Deep Sea Trenches and Back-arc Basins*, *Maurice Ewing Ser.*, vol. 1, edited by M. Talwani and W. C. Pitman III, pp. 1–14, AGU, Washington, D. C.

Uyeda, S., and H. Kanamori (1979), Back-arc opening and the mode of subduction, *J. Geophys. Res.*, *84*, 1049–1061.

Wessel, P., and W. H. F. Smith (1998), New improved version of Generic Mapping Tools released, *Eos Trans. AGU*, *79*, 579.

Zellmer, K., and B. Taylor (2001), A three-plate kinematic model for Lau Basin opening, *Geochem. Geophys. Geosyst.*, *2*(5), doi:10.1029/2000GC000106.